

A geometry-induced topological phase transition in random graphs

Jasper van der Kolk,^{1,2,*} M. Ángeles Serrano,^{1,2,3,†} and Marián Boguñá^{1,2,‡}

¹*Departament de Física de la Matèria Condensada,*

Universitat de Barcelona, Martí i Franquès 1, E-08028 Barcelona, Spain

²*Universitat de Barcelona Institute of Complex Systems (UBICS), Universitat de Barcelona, Barcelona, Spain*

³*Institució Catalana de Recerca i Estudis Avançats (ICREA),
Passeig Lluís Companys 23, E-08010 Barcelona, Spain*

Clustering – the tendency for neighbors of nodes to be connected – quantifies the coupling of a complex network to its underlying latent metric space. In random geometric graphs, clustering undergoes a continuous phase transition, separating a phase with finite clustering from a regime where clustering vanishes in the thermodynamic limit. We prove this geometric-to-nongeometric phase transition to be topological in nature, with atypical features such as diverging free energy and entropy as well as anomalous finite size scaling behavior. Moreover, a slow decay of clustering in the nongeometric phase implies that some real networks with relatively high levels of clustering may be better described in this regime.

Network geometry [1] provides a simple and comprehensive approach to complex networks. The existence of latent metric spaces underlying complex networks offers a deft explanation for their intricate topologies, giving at the same time important clues on their functionality. The small-world property, high levels of clustering (or triangles in the graph), heterogeneity in the degree distribution, and hierarchical organization are all topological properties observed in real networks that find a simple explanation within the network geometry paradigm. In addition, this approach has been used to define geometric communities [2–4], to understand the self-similar architecture of real networks [5–7], the navigability properties of systems such as the Internet [8–10] and the human brain [11], and the temporal evolution of social networks [12].

These results are based on the S^1 model [5] and its isomorphically equivalent formulation, the H^2 model [13]. In the S^1 model, nodes are assumed to live in a metric similarity space where distances can be evaluated. At the same time, nodes are heterogeneous, with popular and not so popular nodes coexisting within the same system. A link between a pair of nodes is created with a probability that resembles a gravity law, increasing with the product of nodes' popularities and decreasing with the increase of their distance in the similarity space. Interestingly, both similarity and popularity coordinates can be combined to map nodes onto the hyperbolic plane so that the connection probability of the S^1 model becomes just a function of the hyperbolic distance among nodes [13]. This allows us to say that hyperbolic geometry is the “natural” geometry of complex networks. Interestingly, many analytic results have been derived for the S^1/H^2 model, e. g. degree distribution [5, 13, 14], clustering [13–15], diameter [16–18], percolation [19, 20], self-similarity [5], or spectral properties [21].

As shown in [13, 22], the S^1/H^2 model is equivalent to a system of noninteracting fermions at temperature T . The fermions correspond to the links of the network and live

on a discrete phase space defined by the $N(N-1)/2$ pairs of distances among the N nodes of the network. Interestingly, despite the fact that fermions in the model are non-interacting particles, we show that the system undergoes a topological phase transition at a critical temperature $T_c = \beta_c^{-1}$, separating a “geometric” phase, with a finite fraction of triangles attached to nodes (clustering), and a nongeometric phase, where clustering vanishes in the thermodynamic limit. This transition is not exclusive to the S^1/H^2 model as it takes place in a very general class of spatial networks defined in compact homogeneous and isotropic Riemannian manifolds of arbitrary dimensionality [22].

In this letter, we analyze in detail this geometric-to-nongeometric (GNG) phase transition which shows interesting anomalous scaling behavior as compared with standard continuous phase transitions, where one observes a power law decay at the critical point and a faster decay in the disordered phase. In fact, the GNG transition is reminiscent of the Berezinskii-Kosterlitz-Thouless topological phase transition (BKT) [23, 24] in the sense that there is no symmetry breaking at the critical point but a transition between two phases with a different organization of topological defects, in this case given by the cycles in the network. However, unlike the BKT transition, the GNG transition is driven by the divergence of both the free energy and the entropy of the system. As a result, in the geometric phase $\beta > \beta_c$, the order parameter measuring clustering approaches continuously the transition with very smooth behavior; at the critical point, the finite size behavior of clustering is anomalous, decaying logarithmically to zero for very large systems; in the nongeometric phase, we discover a weakly geometric region $\beta'_c < \beta < \beta_c$ where clustering decays as a power of the system size with an exponent that depends on the temperature; and finally, when $\beta < \beta'_c$, clustering behaves as in standard random graphs [25]. We show that these results can be interpreted as those of a standard continuous phase transition with an effective

tive system size $N_{\text{eff}} = \ln N$. This leads us to propose the standard finite size scaling hypothesis but with N_{eff} instead of N . Beyond the obvious theoretical interest, these results have practical implications since we show that several real complex networks with high levels of clustering are better described using the $\mathbb{S}^1/\mathbb{H}^2$ model with $\beta \lesssim \beta_c$, thus justifying studying the large temperature behavior.

The \mathbb{S}^1 is a model with hidden variables, representing the location of the nodes in a similarity space and their popularity within the network. Specifically, each node is assigned a random angular coordinate θ_i distributed uniformly in $[0, 2\pi]$, fixing its position in a circle of radius $R = N/2\pi$. In this way, in the limit $N \gg 1$ nodes are distributed in a line according to a Poisson point process of density one with periodic boundary conditions. Each node is also given a hidden degree κ_i , which corresponds to its ensemble expected degree. Each pair of nodes is connected with probability

$$p_{ij} = \frac{1}{1 + \left(\frac{x_{ij}}{\hat{\mu}\kappa_i\kappa_j}\right)^\beta}, \quad (1)$$

where $x_{ij} = R\Delta\theta_{ij}$ is the distance between nodes i and j along the circle, and $\beta > 1$ and $\hat{\mu}$ are model parameters fixing the average clustering coefficient and average degree of the network, respectively. Interestingly, the connection probability in Eq. (1) can be rewritten as the Fermi distribution

$$p_{ij} = \frac{1}{e^{\beta(\varepsilon_{ij}-\mu)} + 1}, \quad (2)$$

where the energy of state ij is

$$\varepsilon_{ij} = \ln \left[\frac{x_{ij}}{\kappa_i\kappa_j} \right] \quad (3)$$

and the chemical potential $\mu = \ln \hat{\mu}$. Then, it becomes clear that the \mathbb{S}^1 model can be thought of as a system of noninteracting identical fermions, corresponding to links, that can occupy the set of $N(N-1)/2$ states with energies given by ε_{ij} , which grow slowly with the distance. In this representation, parameter β plays the role of the inverse of temperature, controlling the level of noise in the system, whereas the chemical potential μ fixes the expected number of links.

In the low temperature regime $\beta > 1$, the chemical potential is $\mu = \ln \left(\frac{\beta}{2\pi\langle k \rangle} \sin \frac{\pi}{\beta} \right)$ [22], with $\langle k \rangle$ the network average degree. Assuming a node distribution on the circle described by a Poisson point process, the free energy per link of the system reads

$$\frac{2F}{N\langle k \rangle} = \ln \left(\frac{\beta}{2\pi\langle k \rangle} \sin \frac{\pi}{\beta} \right) - 1 \quad (4)$$

and the entropy per link

$$\frac{2S}{N\langle k \rangle} = \beta - \pi \cot \frac{\pi}{\beta}, \quad (5)$$

which have been calculated from the grand canonical partition function and the grand potential (see SI). Notice that both the free energy and entropy per link diverge at the critical temperature $\beta = \beta_c = 1$. This implies that there is a phase transition at β_c that is anomalous and cannot be described by Landau's symmetry-breaking theory of continuous phase transitions [26] and, thus, the order parameter cannot be defined as a derivative of the free energy. We conjecture that, as the underlying mechanisms leading to this anomalous behavior are quite general, these findings are not exclusive to the \mathbb{S}^1 model.

We argue that β_c separates two distinct phases with different organization of the cycles in the network. More specifically, a geometric phase with finite clustering corresponds to $\beta > \beta_c$, where the triangle inequality induces a finite fraction of triangles attached to nodes, and a nongeometric phase with zero clustering in the thermodynamic limit is reached when $\beta < \beta_c$, where links are mainly long range and the fraction of triangles vanish. This indicates that clustering is a useful order parameter to characterize this transition, and that the emergence of clustering conditions the abundance of long range connections. At low temperatures, the high energy associated to connecting spatially distant points causes the majority of links attached to a given node to be local. The number of energetically feasible links connecting very distant pairs of nodes grows as temperature increases, diverging at the critical point when $\beta \rightarrow \beta_c^+$ and causing the divergence of the entropy, which is a measure of the number of effective link microstates. At $\beta \leq \beta_c$ the number of available long range states becomes suddenly macroscopic due to the logarithmic dependence of the energy on the distance, which causes the divergence of the entropy in this regime.

In the high temperature regime $\beta < \beta_c$, for a fixed set of coordinates (κ_i, θ_i) , the \mathbb{S}^1 model can be defined in different ways depending on the specific constraints and how the connection probability depends on distance (while still being geometric and maximally random). If we fix the sequence of expected degrees, so that the degree distribution of the network remains unaltered when temperature is increased beyond the critical temperature, the connection probability is [22] should be

$$p_{ij} = \frac{1}{1 + \frac{x_{ij}^\beta}{\hat{\mu}\kappa_i\kappa_j}}, \quad (6)$$

with $\hat{\mu} \approx (1 - \beta)2^{-\beta}N^{\beta-1}/\langle k \rangle$ for $\beta < 1$ and $\hat{\mu} = (2\langle k \rangle \ln N)^{-1}$ when $\beta = 1$. Notice that the model converges to the soft configuration model with a given expected degree sequence [25, 27–29] in the limit of infinite temperature $\beta = 0$. As an alternative, one could use the same connection probability in Eq. (1) and fix the value of $\hat{\mu}$ taking into account the finite size of the system. In this case, the degree distribution becomes progressively more homogeneous as the temperature increases, converging to the Erdos-Renyi ensemble $\mathcal{G}(N, p)$ [30] with $p \sim N^{-1}$ in

the infinite temperature limit. In both definitions, the long range connections become ubiquitous, which causes the entropy density to diverge and the clustering vanish in the thermodynamic limit. In the following, we use the first approach because, by fixing the degree sequence, the model can be directly compared with real networks.

We compute the global clustering coefficient, C , as the local clustering coefficient averaged over all nodes in a network. The local clustering coefficient for a given node i is defined as the probability that a pair of randomly chosen neighbors are neighbors themselves and, using results from [31], it can be computed as

$$C_i = \frac{\sum_{j \neq i} \sum_{k \neq i} p_{ij} p_{jk} p_{ik}}{\left(\sum_{j \neq i} p_{ij}\right)^2}. \quad (7)$$

In the SI we derive analytic results for the behavior of clustering in the neighborhood of the critical point when hidden degrees follow a power law distribution $\rho(\kappa) \sim \kappa^{-\gamma}$ with $2 < \gamma < 3$ and a cutoff $\kappa < \kappa_c \sim N^\alpha$, $\alpha > 1/2$, growing faster than the structural cutoff $\kappa_s \sim N^{1/2}$, which sets the onset of structural degree-degree correlations [32]. Specifically, C behaves as

$$C \sim \begin{cases} (\beta - \beta_c)^2 & \beta > \beta_c \\ [\ln N]^{-2} & \beta = \beta_c \\ N^{-\sigma(\beta)} & \beta'_c < \beta < \beta_c \\ N^{-\sigma(\beta)} \ln N & 0 \leq \beta < \beta'_c \end{cases}, \quad (8)$$

where $\beta'_c = \frac{2}{\gamma}$ and

$$\sigma(\beta) = \begin{cases} 2(\beta^{-1} - 1) & \beta'_c < \beta < \beta_c \\ \gamma - 2 & 0 \leq \beta < \beta'_c \end{cases}. \quad (9)$$

If $\alpha = 1/2$, then the logarithm in the last line of Eq. (8) should be removed and if κ_c grows with N slower than any power law then $\beta'_c = \frac{2}{3}$ and $\sigma(\beta) = 1$ when $\beta < \beta'_c$. See the SI for the general case $\kappa_c \sim N^\alpha$ with $\alpha < 1/2$. Notice that the behavior in a close neighborhood of β_c is independent of γ .

Results in Eq. (8) are remarkable in many respects. First, clustering undergoes a continuous transition at $\beta_c = 1$, attaining a finite value in the geometric phase $\beta > \beta_c$ and becoming zero in the nongeometric phase $\beta < \beta_c$ in the thermodynamic limit. Additionally, the approach to zero when $\beta \rightarrow \beta_c^+$ is very smooth since both clustering and its first derivative are continuous at the critical point. Second, right at the critical point, clustering decays logarithmically with the system size, and it decays as a power of the system size when $\beta < \beta_c$. This is at odds with traditional continuous phase transitions, where one observes a power law decay at the critical point and an even faster decay in the disordered phase. Third, there

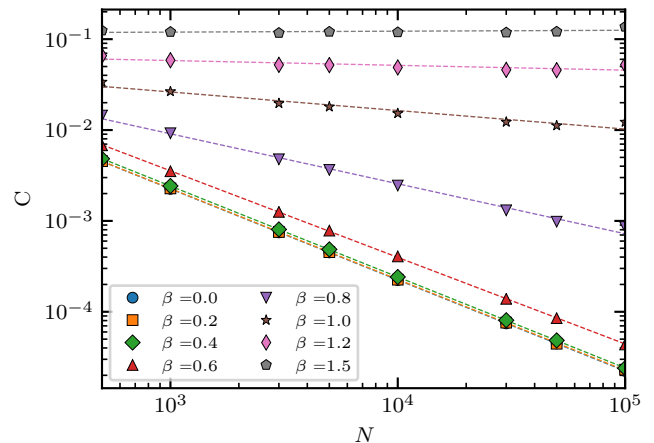


FIG. 1. Average clustering coefficient vs network size for \mathbb{S}^1 geometric networks with homogeneous degrees. The networks were generated by applying the DPG technique to a configuration model network with a homogeneous degree sequence $k = 4, \forall k$. Dashed lines are power law fits used to estimate the exponent σ .

is a weakly geometric region $\beta'_c < \beta < \beta_c$ where clustering decays very slowly, with an exponent that depends on the temperature. Finally, at $\beta < \beta'_c$, we recover the same result of the soft configuration model for scale-free degree distributions [25]. The results in Eq. (8) around the critical point suggest that $N_{\text{eff}} = \ln N$ and not N plays the role of the system size. Indeed, in terms of this effective size, we observe a power law decay at the critical point and a faster decay in the unclustered phase, as expected for a continuous phase transition. Consequently, we expect the finite size scaling ansatz of standard continuous phase transitions to hold with this effective size. We then propose that, in the neighborhood of the critical point, clustering at finite size N can be written as

$$C(\beta, N) = [\ln N]^{-\frac{\eta}{\nu}} f\left((\beta - \beta_c) [\ln N]^{\frac{1}{\nu}}\right), \quad (10)$$

with $\eta = 2$, $\nu = 1$, and where $f(x)$ is a scaling function that behaves as $f(x) \sim x^\eta$ for $x \rightarrow \infty$.

We test these results with numerical simulations, and by direct numerical integration of Eq. (7) using Eq. (1) for $\beta > \beta_c$ and Eq. (6) for $\beta \leq \beta_c$, see SI. Simulations are performed with the degree-preserving geometric Metropolis-Hastings algorithm (DPG) introduced in [33], that allows us to explore different values of β while preserving exactly the degree sequence. Given a network, the algorithm selects at random a pair of links connecting nodes i, j and l, m and swaps them (avoiding multiple links and self-connections) with a probability given by

$$p_{\text{swap}} = \min \left[1, \left(\frac{\Delta\theta_{ij} \Delta\theta_{lm}}{\Delta\theta_{il} \Delta\theta_{jm}} \right)^\beta \right], \quad (11)$$

where $\Delta\theta$ is the angular separation between the corre-

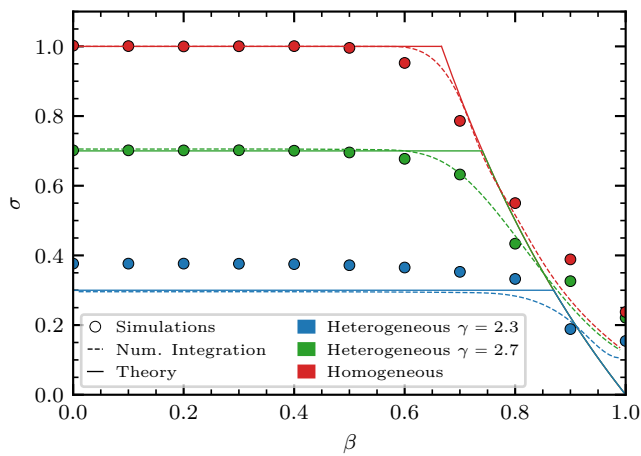


FIG. 2. Exponent σ in the nongeometric phase evaluated from numerical simulations with the DPG algorithm (colored circles), numerical integration of Eq. (7) (dashed lines), and theoretical approach Eq. (8) (solid lines). Networks are generated with a homogeneous distribution of hidden degrees (red lines and circles) and a power law distribution with exponents $\gamma = 2.3$ and $\gamma = 2.7$, blue and green lines and circles, respectively. In the heterogeneous case, we fit a function of the form $N^{-\sigma} \ln N$ when $\beta < 2/\gamma$ to obtain the exponent σ .

sponding pair of nodes. This algorithm maximizes the likelihood that the network is \mathbb{S}^1 geometric while preserving the degree sequence and the set of angular coordinates, and it does so both above and below the critical temperature. Notice that the algorithm does not depend on the hidden degrees κ_i , nor on the parameter $\hat{\mu}$.

Figure 1 shows the behavior of the average clustering coefficient as a function of the number of nodes for homogeneous \mathbb{S}^1 networks with different values of β , showing a clear power law dependence $N^{-\sigma}$ in the nongeometric phase $\beta < \beta_c$, with an exponent that varies with β as predicted by our analysis. These results are used to measure the exponent σ as a function of the inverse temperature β , which in Fig. 2 are compared with the theoretical value given by Eq. (8). The agreement is not very good for values of β close to β_c and for very heterogeneous networks. This discrepancy is expected due to the slow approach to the thermodynamic limit in the nongeometric phase, which suggests that the range of our numerical simulations, $N \in [5 \times 10^2, 10^5]$, is too limited. To test for this possibility, we solve numerically Eq. (7) for sizes in the range $N \in [5 \times 10^5, 10^8]$ and measure numerically the exponent σ . In this case, the agreement is also very good for heterogeneous networks. The remaining discrepancy when $\beta \approx \beta_c$ is again expected since, as shown in Eq. (8), right at the critical point clustering decays logarithmically rather than as a power law. Finally, Fig. 3 shows the finite size scaling Eq. (10) both for the numerical simulations and numerical integration of Eq. (7). In both cases, we find a very good collapse

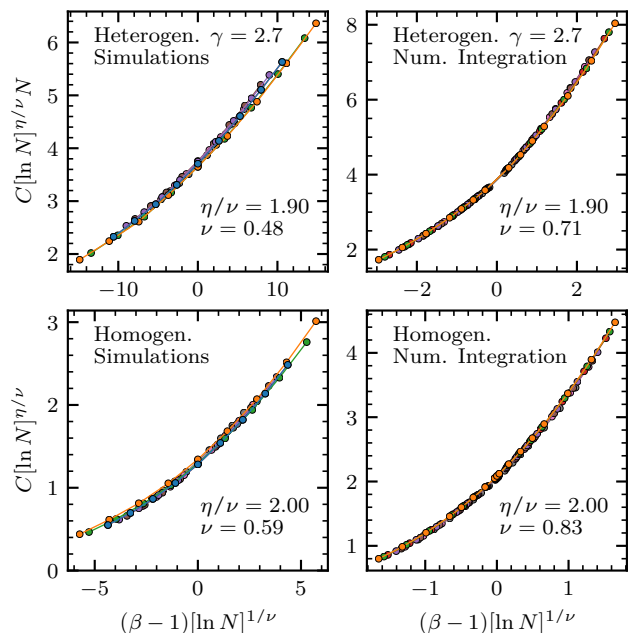


FIG. 3. Finite size scaling Eq. (10) for heterogeneous networks with $\gamma = 2.7$ (top row) and homogeneous networks (bottom row). Left column correspond to numerical simulations with sizes in the range $N \in (5 \times 10^2, 10^5)$, whereas the right column is obtained from numerical integration of Eq. (8) with sizes in the range $N \in (5 \times 10^5, 10^8)$.

with exponent $\eta/\nu \approx 2$ in all cases. The exponent ν , however, departs from the theoretical value $\nu = 1$ in numerical simulations due to their small sizes but improves significantly with numerical integration for bigger sizes. We then expect Eq. (10) to hold, albeit for very large system sizes.

The slow decay of clustering in the nongeometric phase implies that some real networks with significant levels of clustering may be better described using the \mathbb{S}^1 model with temperatures in the regime $\beta < \beta_c$. Given a real network, the DPG algorithm can be used to find its value of β . To do so, nodes in the real network are given random angular coordinates in $(0, 2\pi)$. Then the DPG algorithm is applied, increasing progressively the value of β until the clustering coefficient of the randomized network matches the one measured in the real network. Many real networks have very high levels of clustering and lead to values of $\beta > \beta_c$. However, there are notable examples with values of β below the critical point. As an example, in the SI table we show values of β obtained for several real networks of interest with values below of slightly above β_c . In fact, some of them are found to be very close to the critical point, like protein-protein interaction networks of specific human tissues, with $\beta \approx 1$ or the genetic interaction network of the *Drosophila Melanogaster*, $\beta \approx 1.1$.

Our results in this letter show that the coupling of the

energies of states and an underlying geometry in systems of noninteracting fermions can lead to anomalous phase transitions between different topological phases. Despite fermions being noninteracting, the set of states that these fermions can occupy are correlated by the triangle inequality in the underlying metric space. This correlation then induces an effective interaction between fermions, ultimately leading to a clustered phase at low temperatures. Interestingly, the logarithmic dependence of the energy of states with the metric distance results in the divergence of the free energy and entropy at a finite temperature β_c and, thus, to a different ordering of cycles below β_c , where clustering vanishes in the thermodynamic limit. The finite size behavior of the transition is anomalous, with $\ln N$ and not N playing the role of the system size. Such slow approach to the thermodynamic limit is relevant in real networks in the nongeometric phase, $\beta \lesssim \beta_c$, for which high levels of clustering can still be observed. All together, our results describe an anomalous topological phase transition that cannot be described by the classic Landau theory but that is, nevertheless, different from other topological phase transitions, such as the BKT transition.

ACKNOWLEDGMENTS

We acknowledge support from: the ICREA Academia award, funded by the Generalitat de Catalunya; Agencia estatal de investigación project number PID2019-106290GB-C22/AEI/10.13039/501100011033; and Generalitat de Catalunya grant number 2017SGR1064. J. vd K. acknowledges support from the Secretaria d'Universitats i Recerca de la Generalitat de Catalunya i del Fons Social Europeu.

* jasper.vanderkolk@ub.edu

† marian.serrano@ub.edu

‡ marian.boguna@ub.edu

- [1] M. Boguna, I. Bonamassa, M. D. Domenico, S. Havlin, D. Krioukov, and M. A. Serrano, *Nature Reviews Physics* **3**, 114 (2021), [arXiv:2001.03241](https://arxiv.org/abs/2001.03241) [physics.soc-ph].
- [2] M. Á. Serrano, M. Boguñá, and F. Sagués, *Mol Biosyst* **8**, 843 (2012).
- [3] G. García-Pérez, M. Boguñá, A. Allard, and M. A. Serrano, *Scientific Reports* **6**, 33441 (2016).
- [4] A. Faqeeh, S. Osat, and F. Radicchi, *Phys Rev Lett* **121**, 098301 (2018).
- [5] M. Á. Serrano, D. Krioukov, and M. Boguñá, *Phys Rev Lett* **100**, 078701 (2008).

- [6] G. García-Pérez, M. Boguñá, and M. Á. Serrano, *Nature Physics* **2018** **14**, 583 (2018).
- [7] M. Zheng, A. Allard, P. Hagmann, Y. Alemán-Gómez, and M. Á. Serrano, *Proceedings of the National Academy of Sciences* **117**, 20244 (2020).
- [8] M. Boguñá, D. Krioukov, and K. C. Claffy, *Nat Phys* **5**, 74 (2009).
- [9] M. Boguñá, F. Papadopoulos, and D. Krioukov, *Nat Commun* **1**, 1 (2010).
- [10] A. Gulyás, J. J. Bíró, A. Kőrösi, G. Rétvári, and D. Krioukov, *Nat Commun* **6**, 7651 (2015).
- [11] A. Allard and M. Á. Serrano, *PLOS Computational Biology* **16**, e1007584 (2020).
- [12] M. A. R. Flores and F. Papadopoulos, *Physical review letters* **121**, 258301 (2018).
- [13] D. Krioukov, F. Papadopoulos, M. Kitsak, A. Vahdat, and M. Boguñá, *Phys Rev E* **82**, 036106 (2010).
- [14] L. Gugelmann, K. Panagiotou, and U. Peter, in *Autom Lang Program (ICALP 2012, Part II)*, *LNCS 7392* (2012).
- [15] E. Candellero and N. Fountoulakis, *Internet Math* **12**, 2 (2016).
- [16] M. A. Abdullah, N. Fountoulakis, and M. Bode, *Internet Math* **10.24166/im.13.2017** (2017).
- [17] T. Friedrich and A. Krohmer, *SIAM J Discret Math* **32**, 1314 (2018).
- [18] T. Müller and M. Staps, *Adv Appl Probab* **51**, 358 (2019).
- [19] M. Á. Serrano, D. Krioukov, and M. Boguñá, *Phys Rev Lett* **106**, 048701 (2011).
- [20] N. Fountoulakis and T. Müller, *Ann Appl Probab* **28**, 607 (2018).
- [21] M. Kiwi and D. Mitsche, *Ann Appl Probab* **28**, 941 (2018).
- [22] M. Boguñá, D. Krioukov, P. Almagro, and M. A. Serrano, *Phys. Rev. Research* **2**, 023040 (2020).
- [23] V. Berezinskii, *Sov. Phys. JETP* **32**, 493 (1971); **34**, 610 (1972).
- [24] J. M. Kosterlitz and D. J. Thouless, *Journal of Physics C: Solid State Physics* **6**, 1181 (1973).
- [25] P. Colomer-de Simón and M. Boguñá, *Phys Rev E* **86**, 026120 (2012).
- [26] P. Hohenberg and A. Krekhov, *Physics Reports* **572**, 1 (2015), an introduction to the Ginzburg–Landau theory of phase transitions and nonequilibrium patterns.
- [27] J. Park and M. E. J. Newman, *Phys Rev E* **70**, 66117 (2004).
- [28] P. van der Hoorn, G. Lippner, and D. Krioukov, *Journal of Statistical Physics* **173**, 806 (2018).
- [29] D. Garlaschelli, F. Den Hollander, and A. Roccaverde, *Journal of Statistical Physics* **173**, 644 (2018).
- [30] P. Erdős and A. Rényi, *Publ Math* **6**, 290 (1959).
- [31] M. Boguñá and R. Pastor-Satorras, *Phys Rev E* **68**, 36112 (2003).
- [32] M. Boguñá, R. Pastor-Satorras, and A. Vespignani, *Eur Phys J B - Condens Matter* **38**, 205 (2004).
- [33] M. Starnini, E. Ortiz, and M. Á. Serrano, *New Journal of Physics* **21**, 053039 (2019).

Supplementary Information for A geometry-induced topological phase transition in random graphs

Jasper van der Kolk,^{1,2,*} M. Ángeles Serrano,^{1,2,3,†} and Marián Boguñá^{1,2,‡}

¹*Departament de Física de la Matèria Condensada,*

Universitat de Barcelona, Martí i Franquès 1, E-08028 Barcelona, Spain

²*Universitat de Barcelona Institute of Complex Systems (UBICS), Universitat de Barcelona, Barcelona, Spain*

³*Institució Catalana de Recerca i Estudis Avançats (ICREA),*

Passeig Lluís Companys 23, E-08010 Barcelona, Spain

CONTENTS

I. Analytics	1
A. Preliminaries	1
B. Free Energy and Entropy	3
C. Scaling Behaviour of Clustering with System Size	3
1. Angular Manipulation	4
2. Case $0 < \beta < 1$	5
3. Case $\beta = 1$	11
D. Exponent η	15
II. Real Networks	16
References	16

I. ANALYTICS

A. Preliminaries

The average clustering coefficient for a node with hidden degree κ and angular position θ is defined in the \mathbb{S}^1 [1] model as

$$C(\kappa, \theta) = \left(\frac{N}{\bar{k}(\kappa, \theta)} \right)^2 \int d\kappa' d\kappa'' d\theta' d\theta'' \rho(\kappa') \rho(\kappa'') F(\kappa', \kappa'', \theta', \theta'') F(\kappa, \kappa'', \theta, \theta'') F(\kappa, \kappa', \theta, \theta'), \quad (\text{S1})$$

in a network with system size N . Here the function $\bar{k}(\kappa, \theta)$ is the average degree of a node with hidden coordinates (κ, θ) , $\rho(\kappa)$ is the hidden degree density and $F(\kappa, \kappa', \theta, \theta')$ is the connection probability between two nodes with hidden coordinates (κ, θ) and (κ', θ') . The exact form of these functions will be discussed in the following. Note that as the model has rotation symmetry, one only needs to investigate the node at angular coordinate $\theta = 0$. The average clustering coefficient can be computed from $C(\kappa)$ in the following manner

$$C = \int d\kappa' \rho(\kappa') C(\kappa'). \quad (\text{S2})$$

However, as $C(\kappa)$ is a bounded monotonically decreasing function, it suffices to find the scaling of $C(\kappa)$ for small κ [2]. In Eq. (S1), $\rho(\kappa)$ defines the distribution of the hidden degrees. In the following, we always apply a power law distribution. As we are interested in finite-sized scale-free networks, we choose the following distribution

$$\rho(\kappa) = \frac{(\gamma - 1) \kappa_0^{\gamma-1}}{1 - \left(\frac{\kappa_c}{\kappa_0} \right)^{1-\gamma}} \kappa^{-\gamma} \quad \kappa_0 < \kappa < \kappa_c. \quad (\text{S3})$$

* jasper.vanderkolk@ub.edu

† marian.serrano@ub.edu

‡ marian.boguena@ub.edu

We choose to not specify the specific form of the cut-offs just yet. We just demand that κ_0 is such that the correct average degree is obtained and that, to lowest order, it does not depend on the system size. The average degree of nodes with hidden variable κ and angular position θ is defined as

$$\bar{k}(\kappa, \theta) = N \int d\kappa' d\theta' \rho(\kappa') F(\kappa, \kappa', \theta, \theta'). \quad (\text{S4})$$

The function F describes the probability of two nodes in the network to be connected and is given by the Fermi-Dirac distribution. As was proved in Ref. [3], the exact form of this function is different for β above and below one. For high temperatures, $\beta < 1$,

$$F(\kappa', \kappa'', \theta', \theta'') = \frac{1}{1 + \frac{(N\Delta\theta)^\beta}{(2\pi)^\beta \hat{\mu} \kappa' \kappa''}}. \quad (\text{S5})$$

Here $\Delta\theta = \pi - |\pi - |\theta' - \theta''||$. The quantity $\hat{\mu}$ in 1D in this region is given by

$$\hat{\mu}(N) = \frac{(1 - \beta)}{2^\beta \langle k \rangle N^{1-\beta}}. \quad (\text{S6})$$

The quantity $\hat{\mu}$ in our model controls the degree distribution of the system. As was explained in the main text, we want the distribution to remain constant when varying β , which is why one needs to introduce different connection probabilities and redefine $\hat{\mu}$ for the different regimes. For low temperatures, $\beta > 1$, we can follow the same logic as was used to derive Eq. (S5) to find

$$F(\kappa', \kappa'', \theta', \theta'') = \frac{1}{1 + \left(\frac{N\Delta\theta}{2\pi \hat{\mu} \kappa' \kappa''} \right)^\beta}. \quad (\text{S7})$$

In Ref. [3] it is noted that in this regime one can also define a connection probability in the thermodynamic limit, given in terms of the spatial coordinates x , in our 1D case the coordinates on a infinite line:

$$F_{N \rightarrow \infty}(\kappa', \kappa'', x', x'') = \frac{1}{1 + \left(\frac{|x' - x''|}{\hat{\mu} \kappa' \kappa''} \right)^\beta}, \quad (\text{S8})$$

In both Eq. (S8) and (S7) $\hat{\mu}$ is given by

$$\hat{\mu} = \frac{\beta \sin(\pi/\beta)}{2\pi \langle k \rangle}. \quad (\text{S9})$$

Exactly at the transition point $\hat{\mu}$ also takes a different form. As in Ref. [3] this specific case was not investigated we derive it here. One starts with an expression for the expected degree κ .

$$\begin{aligned} \kappa &= \frac{N}{\pi} \int d\alpha' \rho(\alpha') \int_0^\pi \frac{d\theta}{1 + \frac{N\theta}{2\pi} \exp(\alpha + \alpha')} \\ &= 2 \int d\alpha' \rho(\alpha') \exp(-\alpha - \alpha') \int_1^{1 + \frac{N}{2} \exp(\alpha + \alpha')} \frac{dt}{t} \\ &= 2 \int d\alpha' \rho(\alpha') \exp(-\alpha - \alpha') \ln \left(1 + \frac{N}{2} \exp(\alpha + \alpha') \right). \end{aligned} \quad (\text{S10})$$

Now, for large system sizes one obtains

$$\kappa = 2 \ln(N) \int d\alpha' \rho(\alpha') \exp(-\alpha - \alpha') = 2 \ln(N) \exp(-\alpha) \langle \exp(-\alpha) \rangle. \quad (\text{S11})$$

Using that $\langle \kappa \rangle = \langle k \rangle$, we have

$$\langle k \rangle = 2 \ln(N) \langle \exp(-\alpha) \rangle^2, \quad (\text{S12})$$

which implies that

$$\kappa = (2\langle k \rangle \ln(N))^{1/2} \exp(-\alpha) \Rightarrow \alpha = -\left(\ln(\kappa) + \frac{1}{2} \ln\left(\frac{1}{2\langle k \rangle \ln(N)}\right)\right) \quad (\text{S13})$$

Using now that $\alpha = -(\ln \kappa + \frac{1}{2} \ln \hat{\mu})[3]$ and $\hat{\mu} = \exp \mu$ one finally finds

$$\hat{\mu} = \left(2\langle k \rangle \ln(N)\right)^{-1}. \quad (\text{S14})$$

B. Free Energy and Entropy

As was explained in the main text, for $\beta > 1$, the edges can be taken to represent noninteracting fermions with energy equal to

$$\epsilon_{ij} = \ln \left[\frac{x_{ij}}{\kappa_i \kappa_j} \right]. \quad (\text{S15})$$

One can then define the grand canonical partition function of the system as follows

$$\ln \mathcal{Z} = \sum_{i,j} \ln \left[1 + \left(\frac{x_{ij}}{\hat{\mu} \kappa_i \kappa_j} \right)^{-\beta} \right], \quad (\text{S16})$$

where $\hat{\mu} = \exp \mu$, with μ the chemical potential. Now, as similarity space is homogeneous, one can place the i 'th node on the origin, leading to N identical terms. Then we assume to be working with a large system size allowing us to approximate the sums in Eq. (S16) by integrals. This leads to the following expression

$$\begin{aligned} \ln \mathcal{Z} &= N \iint d\kappa d\kappa' \rho(\kappa) \rho(\kappa') \int dx \ln \left[1 + \left(\frac{x}{\hat{\mu} \kappa \kappa'} \right)^{-\beta} \right] \\ &= N \hat{\mu} \iint d\kappa d\kappa' \rho(\kappa) \rho(\kappa') \kappa \kappa' \int dt \ln [1 + t^{-\beta}] \\ &= N \frac{\hat{\mu} \langle k \rangle^2 \pi}{\sin \frac{\pi}{\beta}} = \frac{N \beta \langle k \rangle}{2}, \end{aligned} \quad (\text{S17})$$

where in the last step $\hat{\mu}$ was plugged in. Note that the expressions is multiplied with a factor N , which of course makes our quantities diverge in the thermodynamic limit. However, it is not the thermodynamic quantities themselves but their densities we are interested in, thus we can divide away the factor N . In fact, we choose to look at the thermodynamic quantities per link, where the amount of links in the system is $N\langle k \rangle/2$. We can then use the above expression to define the grand potential

$$\Xi = -\frac{1}{\beta} \ln \mathcal{Z} = -\frac{1}{2} N \langle k \rangle, \quad (\text{S18})$$

which can in turn be used to find the free energy of the system

$$\frac{2F}{N\langle k \rangle} = \frac{2\Xi}{N\langle k \rangle} + \mu = \mu - 1 = \ln \left(\frac{\beta}{2\pi\langle k \rangle} \sin \frac{\pi}{\beta} \right) - 1 \stackrel{\beta \rightarrow \beta_c^+}{\sim} \ln(\beta - 1) \quad (\text{S19})$$

From this, we can find the entropy of the system

$$\frac{2S}{N\langle k \rangle} = \frac{2\beta^2}{N\langle k \rangle} \frac{\partial F}{\partial \beta} = \beta - \pi \cot \frac{\pi}{\beta} \stackrel{\beta \rightarrow \beta_c^+}{\sim} \frac{1}{\beta - 1}. \quad (\text{S20})$$

C. Scaling Behaviour of Clustering with System Size

In the following section we find the dominant finite size scaling of the clustering coefficient for $\beta \leq 1$. Note that for $\beta > 1$ we already know that clustering is independent of system size as the connection probability is finite in thermodynamic limit. We will look at the properties of this regime in section (ID). We start by manipulating the angular integrals of Eq. (S1) as to simplify the task at hand later on. We then turn to the scaling when $\beta < 1$ and conclude with an analysis of the scaling when $\beta = 1$.

1. Angular Manipulation

We start by manipulating the angular integrals of Eq. (S1) to make it easier to work with, i.e. get rid of the absolute values in the expressions for $\Delta\theta$. The equation has the following form:

$$C(\kappa) = \frac{\iiint d\kappa' d\kappa'' d\theta' d\theta'' \rho(\kappa') \rho(\kappa'') F(\kappa, \kappa', \pi - |\pi - |\theta''||) F(\kappa, \kappa'', \pi - |\pi - |\theta''||) F(\kappa', \kappa'', \pi - |\pi - |\theta' - \theta''||)}{\iint d\kappa' d\theta' \rho(\kappa') F(\kappa, \kappa', \pi - |\pi - |\theta''||)}. \quad (\text{S21})$$

Here, we have used $\theta = 0$. Let us first investigate the trivial case of the denominator, where we only focus on the angular integral

$$\begin{aligned} \int_0^{2\pi} d\theta' F(\kappa, \kappa', \pi - |\pi - |\theta''||) &= \int_0^\pi d\theta' F(\kappa, \kappa', \pi - |\pi - |\theta''||) + \int_\pi^{2\pi} d\theta' F(\kappa, \kappa', \pi - |\pi - |\theta''||) \\ &= \int_0^\pi d\theta' F(\kappa, \kappa', \theta') + \int_\pi^{2\pi} d\theta' F(\kappa, \kappa', 2\pi - \theta') = 2 \int_0^\pi d\theta' F(\kappa, \kappa', \theta'), \end{aligned} \quad (\text{S22})$$

where in the last step we have performed the transformation $t = 2\pi - \theta'$ and $t \rightarrow \theta'$ on the second integral. The numerator can be rewritten in a similar way to obtain four terms

$$\begin{aligned} &\int_0^{2\pi} d\theta' \int_0^{2\pi} d\theta'' F(\kappa, \kappa', \pi - |\pi - |\theta''||) F(\kappa, \kappa'', \pi - |\pi - |\theta''||) F(\kappa', \kappa'', \pi - |\pi - |\theta' - \theta''||) \\ &= 2 \int_0^\pi d\theta' \left(\int_0^{\theta'} d\theta'' F(\kappa, \kappa', \theta') F(\kappa, \kappa'', \theta'') F(\kappa', \kappa'', \theta' - \theta'') + \int_0^{\theta'} d\theta'' F(\kappa, \kappa', \theta'') F(\kappa, \kappa'', \theta') F(\kappa', \kappa'', \theta' - \theta'') \right) \\ &+ \int_0^{\pi - \theta'} d\theta'' F(\kappa, \kappa', \theta') F(\kappa, \kappa'', \theta'') F(\kappa', \kappa'', \theta' + \theta'') + \int_{\pi - \theta'}^\pi d\theta'' F(\kappa, \kappa', \theta') F(\kappa, \kappa'', \theta'') F(\kappa', \kappa'', 2\pi - \theta' - \theta''). \end{aligned} \quad (\text{S23})$$

The first two terms are not exactly the same. However, as the full expression of the clustering coefficient also contains integrals over the hidden degrees, one can interchange $\kappa' \leftrightarrow \kappa''$ together with $\theta' \leftrightarrow \theta''$. This thus shows that the first two terms contribute equally to the clustering coefficient. All in all, we will thus be working with the following three terms

$$\begin{aligned} &4 \int_0^\pi d\theta' \int_0^{\theta'} d\theta'' F(\kappa, \kappa', \theta') F(\kappa, \kappa'', \theta'') F(\kappa', \kappa'', \theta' - \theta'') \\ &+ 2 \int_0^\pi d\theta' \int_0^{\pi - \theta'} d\theta'' F(\kappa, \kappa', \theta') F(\kappa, \kappa'', \theta'') F(\kappa', \kappa'', \theta' + \theta'') \\ &+ 2 \int_0^\pi d\theta' \int_{\pi - \theta'}^\pi d\theta'' F(\kappa, \kappa', \theta') F(\kappa, \kappa'', \theta'') F(\kappa', \kappa'', 2\pi - \theta' - \theta''). \end{aligned} \quad (\text{S24})$$

Now, before we get started on finding the scaling with respect to the system size of each term individually, it might be that we can avoid doing so by some simple arguments. Indeed, we will show that the first term will always dominate the others in the large N limit, and so we only have to find its scaling. Let us start with the second term

$$\begin{aligned} &2 \iint d\kappa' d\kappa'' \rho(\kappa') \rho(\kappa'') \int_0^\pi d\theta' \int_0^{\pi - \theta'} d\theta'' F(\kappa, \kappa', \theta') F(\kappa, \kappa'', \theta'') F(\kappa', \kappa'', \theta' + \theta'') \\ &\leq 2 \iint d\kappa' d\kappa'' \rho(\kappa') \rho(\kappa'') \int_0^\pi d\theta' \int_0^\pi d\theta'' F(\kappa, \kappa', \theta') F(\kappa, \kappa'', \theta'') F(\kappa', \kappa'', \theta' + \theta''). \end{aligned} \quad (\text{S25})$$

The above statement is true as the integrand is strictly positive and so extending the integration domain will only make the integral larger. Now, we can split the θ'' integral and perform $\theta' \leftrightarrow \theta''$ and $\kappa' \leftrightarrow \kappa''$ on the second term to obtain

$$\begin{aligned} &2 \iint d\kappa' d\kappa'' \rho(\kappa') \rho(\kappa'') \int_0^\pi d\theta' \int_0^\pi d\theta'' F(\kappa, \kappa', \theta') F(\kappa, \kappa'', \theta'') F(\kappa', \kappa'', \theta' + \theta'') \\ &= 4 \iint d\kappa' d\kappa'' \rho(\kappa') \rho(\kappa'') \int_0^\pi d\theta' \int_0^{\theta'} d\theta'' F(\kappa, \kappa', \theta') F(\kappa, \kappa'', \theta'') F(\kappa', \kappa'', \theta' + \theta'') \end{aligned}$$

$$\leq 4 \iint d\kappa' d\kappa'' \rho(\kappa') \rho(\kappa'') \int_0^\pi d\theta' \int_0^{\theta'} d\theta'' F(\kappa, \kappa', \theta') F(\kappa, \kappa'', \theta'') F(\kappa', \kappa'', \theta' - \theta''). \quad (\text{S26})$$

In the final step we use the functional form of F with respect to the angular coordinate is

$$F(x) = \frac{1}{1 + x^\beta}. \quad (\text{S27})$$

As x^β is monotonously increasing, and $1/(1+x)$ is monotonously decreasing, $F(x)$ is monotonously decreasing. Thus, it is largest when x is smallest. Obviously, $\theta' + \theta'' > \theta' - \theta''$ for all $(\theta', \theta'') \in [0, \pi] \times [0, \theta']$. We have thus proven that the first term in Eq. (S24) dominates the second term. We can follow similar steps for the third term. We will now only clarify steps if they are new.

$$\begin{aligned} & 2 \iint_{\kappa', \kappa''} d\kappa' d\kappa'' \rho(\kappa') \rho(\kappa'') \int_0^\pi d\theta' \int_{\pi-\theta'}^\pi d\theta'' F(\kappa, \kappa', \theta') F(\kappa, \kappa'', \theta'') F(\kappa', \kappa'', 2\pi - \theta' - \theta'') \\ & \leq 4 \iint_{\kappa', \kappa''} d\kappa' d\kappa'' \rho(\kappa') \rho(\kappa'') \int_0^\pi d\theta' \int_0^{\theta'} d\theta'' F(\kappa, \kappa', \theta') F(\kappa, \kappa'', \theta'') F(\kappa', \kappa'', 2\pi - \theta' - \theta''). \end{aligned} \quad (\text{S28})$$

Now, one knows that $2\pi - \theta' - \theta'' \geq \theta' - \theta'' \forall (\theta', \theta'') \in [0, \pi] \times [0, \theta']$. For the same reasons as before, this then implies

$$\begin{aligned} & 4 \iint_{\kappa', \kappa''} d\kappa' d\kappa'' \rho(\kappa') \rho(\kappa'') \int_0^\pi d\theta' \int_0^{\theta'} d\theta'' F(\kappa, \kappa', \theta') F(\kappa, \kappa'', \theta'') F(\kappa', \kappa'', 2\pi - \theta' - \theta'') \\ & \leq 4 \iint_{\kappa', \kappa''} d\kappa' d\kappa'' \rho(\kappa') \rho(\kappa'') \int_0^\pi d\theta' \int_0^{\theta'} d\theta'' F(\kappa, \kappa', \theta') F(\kappa, \kappa'', \theta'') F(\kappa', \kappa'', \theta' - \theta''), \end{aligned} \quad (\text{S29})$$

so this term is also dominated by the first term in Eq. (S24).

2. Case $0 < \beta < 1$

The first step is to perform the transformation $x = \frac{\kappa'}{\kappa_s}$ and $y = \frac{\kappa''}{\kappa_s}$, where we define $\kappa_s^2 \equiv N^\beta / ((2\pi)^\beta \hat{\mu})$. This leads to

$$C(\kappa) = 2 \frac{\int_{\kappa_0/\kappa_s}^{\kappa_c/\kappa_s} dx \int_{\kappa_0/\kappa_s}^{\kappa_c/\kappa_s} dy \int_0^\pi d\theta' \int_0^{\theta'} d\theta'' (xy)^{-\gamma} F(\kappa, x, \theta') F(\kappa, y, \theta'') F(x, y, \theta' - \theta'')}{\left(\int_{\kappa_0/\kappa_s}^{\kappa_c/\kappa_s} dx \int_0^\pi d\theta' x^{-\gamma} F(\kappa, x, \theta') \right)^2} + h.o.t., \quad (\text{S30})$$

We investigate the numerator and denominator separately and define

$$A_- = \int_{\kappa_0/\kappa_s}^{\kappa_c/\kappa_s} dx \int_{\kappa_0/\kappa_s}^{\kappa_c/\kappa_s} dy \int_0^\pi d\theta' \int_0^{\theta'} d\theta'' (xy)^{-\gamma} F(\kappa, x, \theta') F(\kappa, y, \theta'') F(x, y, \theta' - \theta''). \quad (\text{S31})$$

$$B = \int_{\kappa_0/\kappa_s}^{\kappa_c/\kappa_s} dx \int_0^\pi d\theta' x^{-\gamma} F(\kappa, x, \theta'). \quad (\text{S32})$$

It is also useful to define

$$A_+ = \int_{\kappa_0/\kappa_s}^{\kappa_c/\kappa_s} dx \int_{\kappa_0/\kappa_s}^{\kappa_c/\kappa_s} dy \int_0^\pi d\theta' \int_0^{\theta'} d\theta'' (xy)^{-\gamma} F(\kappa, x, \theta') F(\kappa, y, \theta'') F(x, y, \theta' + \theta''). \quad (\text{S33})$$

Our investigation will focus on finding upper and lower bounds for these integrals. Using the fact that

$$\frac{1}{1 + \frac{(\theta' + \theta'')^\beta}{xy}} < \frac{1}{1 + \frac{(\theta' - \theta'')^\beta}{xy}}, \quad \forall \theta', \theta'', x, y, \quad (\text{S34})$$

we can conclude that $A_+ < A_-$. As numerical investigation leads us to expect that both have the same scaling, this implies that we do not need to worry about an upper bound for A_+ nor the lower bound for A_- . If the functions $f(N)$ and $g(N)$ in equation

$$f(N) < A_+ < A_- < g(N) \quad (\text{S35})$$

have the same dominant scaling, one can immediately conclude that A_- also has that exact dominant scaling. One might ask why we introduce A_+ in the first place, when in the end we are only interested in the scaling of A_- . The answer to this is that A_+ in general has nicer properties due to the lack of $(\theta' - \theta'')$, as it is thus easier to find a lower bound for it than for A_- .

We start with the simplest integral, the B -term, which can be solved exactly. To this end we first need to rewrite it a bit. By performing two substitutions

$$x' = \frac{\kappa_s}{\kappa_c} x \quad x' \rightarrow x, \quad t = \frac{\theta'}{\pi} \quad t \rightarrow \theta', \quad (\text{S36})$$

one obtains

$$B = \pi \left(\frac{\kappa_c}{\kappa_s} \right)^{1-\gamma} \int_0^1 d\theta' \int_{\kappa_0/\kappa_c}^1 dx \frac{x^{-\gamma}}{1 + \frac{(\pi\theta')^\beta \kappa_s^2}{\kappa_c \kappa x}}. \quad (\text{S37})$$

This then gives the following expression

$$B = \frac{\pi}{(\beta(\gamma-1)-1)(\gamma-1)} \left\{ \begin{aligned} & (\gamma-1)\beta \left(\frac{\kappa_0}{\kappa_s} \right)^{1-\gamma} {}_2F_1 \left[\begin{matrix} 1, 1/\beta \\ 1 + 1/\beta \end{matrix}; -\frac{\pi^\beta \kappa_s^2}{\kappa \kappa_0} \right] \\ & - (\gamma-1)\beta \left(\frac{\kappa_c}{\kappa_s} \right)^{1-\gamma} {}_2F_1 \left[\begin{matrix} 1, 1/\beta \\ 1 + 1/\beta \end{matrix}; -\frac{\pi^\beta \kappa_s^2}{\kappa \kappa_0} \right] \\ & - \kappa_0 \left(\frac{\kappa_0}{\kappa_s} \right)^{1-\gamma} {}_2F_1 \left[\begin{matrix} 1, \gamma-1 \\ \gamma \end{matrix}; -\frac{\pi^\beta \kappa_s^2}{\kappa \kappa_0} \right] \\ & + \kappa_0 \left(\frac{\kappa_c}{\kappa_s} \right)^{1-\gamma} {}_2F_1 \left[\begin{matrix} 1, \gamma-1 \\ \gamma \end{matrix}; -\frac{\pi^\beta \kappa_s^2}{\kappa \kappa_0} \right] \end{aligned} \right\}. \quad (\text{S38})$$

Here, ${}_2F_1 \left[\begin{matrix} a, b \\ c \end{matrix}; z \right]$ is the ordinary hypergeometric function [4] To lowest order, using $\kappa_s \sim \sqrt{N}$, one finds that B then scales as

$$B \sim N^{\frac{\gamma-3}{2}} \quad (\text{S39})$$

Next we turn to the A_+ term. From the form of the standard connection probability given in Eq. (S27), we see that it is smallest when x is largest, which is the case when θ', θ'' are largest, so when they are both π . Plugging this in we obtain

$$\begin{aligned} A_+ & \geq \int dx dy (xy)^{-\gamma} \frac{1}{1 + \frac{\pi^\beta \kappa_s}{\kappa x}} \frac{1}{1 + \frac{\pi^\beta \kappa_s}{\kappa y}} \frac{1}{1 + \frac{(2\pi)^\beta}{xy}} \\ & = \pi^{-3\beta} \left(\frac{\kappa}{\kappa_s} \right)^2 \int dx dy (xy)^{2-\gamma} \frac{1}{1 + \frac{\kappa x}{\pi^\beta \kappa_s}} \frac{1}{1 + \frac{\kappa y}{\pi^\beta \kappa_s}} \frac{1}{1 + \frac{xy}{(2\pi)^\beta}}. \end{aligned} \quad (\text{S40})$$

Now, this is exactly the same integral (with the exception of the π 's, but they will obviously not change scaling) as the one evaluated in Ref. [2]. As was found in the reference, the scaling depends on whether how we set κ_c relative to κ_s . We distinguish two regimes. First there, is the regime where $\kappa_0 \ll \kappa_s \ll \kappa_c$. In this case, the scaling is

$$A_+ \geq c_{+,1} \kappa_s^{-2} \ln(\kappa_c/\kappa_s). \quad (\text{S41})$$

Then there is the region where $\kappa_0 \leq \kappa_c \leq \kappa_s$ ($\kappa_0 \ll \kappa_s$ must be required to hold) where one obtains

$$A_+ \geq c_{+,2} \kappa_s^{2\gamma-8} \kappa_c^{6-2\gamma}. \quad (\text{S42})$$

This, however, does not give the full scaling behaviour, as numerical results show us that for large β there is different scaling. To find where this different scaling comes from we take a step back and look at the full integral A_+ as given in Eq. (S33). One might be tempted to, as in Ref. [2], expand the first two connection probabilities to first order. However, the presence of the angular coordinate makes this impossible. The argument of these connection probabilities has the form $x = \frac{\theta^\beta \kappa_s}{\kappa x}$. It becomes clear that for small enough θ , x no longer is large and the approximation thus breaks down. We thus expect different scaling behaviour to arise as a result of small angular coordinates. To investigate this further, we split the integration domain in a convenient way and investigate the domain $\mathcal{D}_1 = [0, (xy)^{1/\beta}] \times [0, t]$. However, this is only possible in the case that both $\kappa_c \leq \kappa_s$, as only then the angular coordinates remain small for all x and y . For the case that $\kappa_c \gg \kappa_s$ we define the more restrictive domain $\mathcal{D}_2 = [0, (\kappa_0/\kappa_s)^{2/\beta}] \times [0, t]$. Starting with the case $\kappa_c \leq \kappa_s$ one finds

$$\begin{aligned} A_+ &\geq \frac{1}{1+2^\beta} \int dx dy (xy)^{2/\beta-\gamma} \frac{1}{1 + \frac{\kappa_s y}{\kappa}} \frac{1}{1 + \frac{\kappa_s x}{\kappa}} \\ &= \frac{(\kappa_s/\kappa)^{-4/\beta+2\gamma-2}}{1+2^\beta} \left(B_{\frac{\kappa}{\kappa_0+\kappa}} \left[\gamma - \frac{2}{\beta}, 1 - \gamma + \frac{2}{\beta} \right] - B_{\frac{\kappa}{\kappa_c+\kappa}} \left[\gamma - \frac{2}{\beta}, 1 - \gamma + \frac{2}{\beta} \right] \right)^2 \\ &\sim c_{+,s,1} \kappa_s^{-4/\beta+2\gamma-2} + c_{+,s,2} \kappa_s^{-4/\beta+2\gamma-2} \kappa_c^{4/\beta-2\gamma}, \end{aligned} \quad (\text{S43})$$

where $B_z[a, b]$ is the incomplete beta function. For the case $\kappa_c \gg \kappa_s$ one obtains

$$\begin{aligned} A_+ &\geq \left(\frac{\kappa_0}{\kappa_s} \right)^{4/\beta} \int dx dy (xy)^{-\gamma} \frac{1}{1 + \frac{\kappa_s \kappa_0^2}{\kappa x \kappa_s^2}} \frac{1}{1 + \frac{\kappa_s \kappa_0^2}{\kappa y \kappa_s^2}} \frac{1}{1 + \frac{2^\beta \kappa_0^2}{xy \kappa_s^2}} \\ &\approx \left(\frac{\kappa_0}{\kappa_s} \right)^{4/\beta} \int dx dy (xy)^{-\gamma} \sim c_{+,s,3} \kappa_s^{-4/\beta+2\gamma-2}, \end{aligned} \quad (\text{S44})$$

where in the first step it was noted that irrespective of the value of x and y , the argument of the connection probabilities is small.

We now have five different scaling behaviours. Which terms dominate will depend on the value of β as well on κ_c . To quantify how the scaling varies with κ_c we introduce the exponent α such that $\kappa_c \sim N^{\alpha/2}$. The different regimes of κ_c described above correspond to $\alpha \in [0, 1]$ for $\kappa_c \leq \kappa_s$ and $\alpha \in (1, \frac{2}{\gamma-1}]$ for $\kappa_c \gg \kappa_s$. Using these definitions we can conclude that

$$A_+ \geq \begin{cases} C_{+,1} N^{-2/\beta+\gamma-1} + C_{+,2} N^{-1} \ln N & \text{if } \kappa_c \gg \kappa_s \\ N^{-1} \left(C_{+,3} N^{\gamma-2/\beta} + C_{+,4} N^{(1-\alpha)(\gamma-2/\beta)} + C_{+,5} N^{(1-\alpha)(\gamma-3)} \right) & \text{if } \kappa_c \leq \kappa_s \end{cases}, \quad (\text{S45})$$

where $C_{+,i}$ are constants.

Now obviously this is just a lower bound. To show that the clustering indeed scales like this we must also find an upper bound, which we do by turning to the A_- term. We divide the integration domain in two: $\mathcal{D}_s = [0, (\kappa_0/\kappa_s)^{2/\beta}] \times [0, \theta']$ and $\mathcal{D}_l = [(\kappa_0/\kappa_s)^{2/\beta}, \pi] \times [0, \theta']$. We first turn to region \mathcal{D}_l .

$$\begin{aligned} A_{-,l} &= \iint_{\mathcal{D}_l} d\theta' d\theta'' \iint dx dy (xy)^{-\gamma} \frac{1}{1 + \frac{\theta'^\beta \kappa_s}{\kappa x}} \frac{1}{1 + \frac{\theta''^\beta \kappa_s}{\kappa y}} \frac{1}{1 + \frac{(\theta' - \theta'')^\beta}{xy}} \\ &\leq \left(\frac{\kappa}{\kappa_s} \right)^2 \iint_{\mathcal{D}_l} d\theta' d\theta'' \iint dx dy (xy)^{2-\gamma} (\theta' \theta'' (\theta' - \theta''))^{-\beta} \frac{1}{1 + \frac{xy}{(\theta' - \theta'')^\beta}} \end{aligned}$$

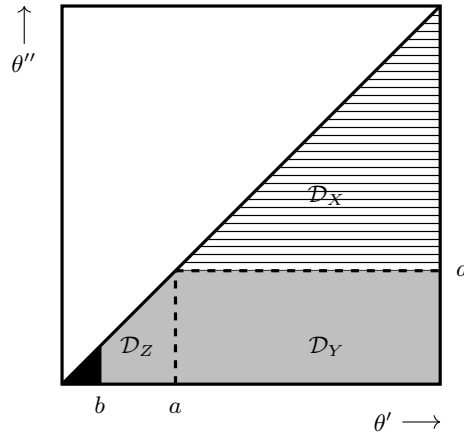


FIG. S1. Integration regions. In the grey region ($\mathcal{D}_Y + \mathcal{D}_Z$) the argument of the Lerch zeta function is bigger than one, in the hatched region (\mathcal{D}_X) it is not and the black region is \mathcal{D}_s .

$$\begin{aligned}
&= \left(\frac{\kappa}{\kappa_s}\right)^2 \iint_{\mathcal{D}_I} \frac{d\theta' d\theta''}{(\theta' \theta'' (\theta' - \theta''))^\beta} \left(\frac{\kappa_c}{\kappa_s}\right)^{2(3-\gamma)} \Phi \left[-(\theta' - \theta'')^{-\beta} \left(\frac{\kappa_c}{\kappa_s}\right)^2, 2, 3 - \gamma \right] \\
&+ \left(\frac{\kappa}{\kappa_s}\right)^2 \iint_{\mathcal{D}_I} \frac{d\theta' d\theta''}{(\theta' \theta'' (\theta' - \theta''))^\beta} \left(\frac{\kappa_0}{\kappa_s}\right)^{2(3-\gamma)} \Phi \left[-(\theta' - \theta'')^{-\beta} \left(\frac{\kappa_0}{\kappa_s}\right)^2, 2, 3 - \gamma \right] \\
&- 2 \left(\frac{\kappa}{\kappa_s}\right)^2 \iint_{\mathcal{D}_I} \frac{d\theta' d\theta''}{(\theta' \theta'' (\theta' - \theta''))^\beta} \left(\frac{\kappa_0 \kappa_c}{\kappa_s^2}\right)^{3-\gamma} \Phi \left[-(\theta' - \theta'')^{-\beta} \frac{\kappa_0 \kappa_c}{\kappa_s^2}, 2, 3 - \gamma \right]. \tag{S46}
\end{aligned}$$

Here, $\Phi[z, a, b]$ is the Lerch zeta function. One sees that these three terms are similar, and so we treat the general integral

$$I_\zeta = \iint_{\mathcal{D}_I} d\theta' d\theta'' \frac{\Phi[-(\theta' - \theta'')^{-\beta} \zeta, 2, 3 - \gamma]}{(\theta' \theta'' (\theta' - \theta''))^\beta} \zeta^{3-\gamma} = \iint_{\mathcal{D}_I} d\theta' d\theta'' \frac{\Phi[-\theta''^{-\beta} \zeta, 2, 3 - \gamma]}{(\theta' \theta'' (\theta' - \theta''))^\beta} \zeta^{3-\gamma}, \tag{S47}$$

where the transformation $\theta''' = \theta' - \theta''$, $\theta''' \rightarrow \theta''$ was performed. Now, the argument of the Lerch zeta function can in principle be smaller and larger than one. If it is smaller, it can be shown that $\Phi[-(\theta' - \theta'')^{-\beta} \zeta, 2, 3 - \gamma] < 2^{\gamma-3}$. If it is bigger one can use the identity described in Ref. [2]

$$\Phi[-z^2, 2, 3 - \gamma] = z^{-2(3-\gamma)} \left(2\psi(\gamma) \ln z + \vartheta(\gamma) \right) + \frac{1}{z^2} \Phi \left[\frac{1}{z^2}, 2, \gamma - 2 \right], \tag{S48}$$

where

$$\psi(\gamma) = \Phi[-1, 1, 3 - \gamma] + \Phi[-1, 1, \gamma - 2] \quad \text{and} \quad \vartheta(\gamma) = -\pi^2 \cot(\pi\gamma) \csc(\pi\gamma). \tag{S49}$$

The transition point between these two cases of course lies at

$$a = \zeta^{1/\beta} \tag{S50}$$

We must thus split the integration domain \mathcal{D}_I in three regions (where $b = (\kappa_0/\kappa_s)^{2/\beta}$): $\mathcal{D}_X = [a, \pi] \times [a, \theta']$, $\mathcal{D}_Y = [a, \pi] \times [0, a]$ and $\mathcal{D}_Z = [b, a] \times [0, \theta']$ as depicted in Fig. S1. Now, the grey region is the one where the Lerch zeta function argument is bigger than one, in the hatched region we can bound the Lerch zeta function away and the black region is \mathcal{D}_s and we thus do not care about it for the moment. Before going any further, let us note that Fig. S1 looks slightly different for different κ_c and ζ . If $\kappa_c \gg \kappa_s$ and $\zeta = (\kappa_c/\kappa_s)^2$, then $\zeta \gg 1$ and thus so is a . However, a as an integration limit must be smaller than π and thus in this case the \mathcal{D}_X and \mathcal{D}_Y regions disappear. When $\kappa_c \leq \kappa_s$ this is not the case as for all ζ , $a < \pi$. Finally, irrespective of the value of κ_c , for $\zeta = (\kappa_0/\kappa_s)^2$, $a = b$ and thus region \mathcal{D}_Z vanishes. Implementing the transformation given by Eq. (S48) in the grey region one obtains

$$I_\zeta \leq \iint d\theta' d\theta'' (\theta' (\theta' - \theta''))^{-\beta} \left\{ \theta''^{\beta(2-\gamma)} \left[\psi(\gamma) \ln \left(\frac{\zeta}{\theta''^\beta} \right) + \vartheta(\gamma) \right] + \zeta^{2-\gamma} (\gamma - 2)^{-2} \right\}. \tag{S51}$$

As this leads to three different angular integrals, in the end we have seven different integrals to solve.

$$\begin{aligned} \iint_{\mathcal{D}_X} d\theta' d\theta'' \left(\frac{1}{\theta' \theta'' (\theta' - \theta'')} \right)^\beta &= \frac{a^{2-3\beta}}{3\beta-2} \left\{ B_1[2\beta-1, 1-\beta] - B_1[1-\beta, 1-\beta] \right. \\ &\quad \left. + B_{\frac{a}{\pi}}[2\beta-1, 1-\beta] + (a/\pi)^{3\beta-2} B_{\frac{a}{\pi}}[1-\beta, 1-\beta] \right\} \\ &\quad + \frac{4^{\beta-1/2} \pi^{5/2-3\beta} \Gamma[1-\beta]}{\Gamma[3/2-\beta](3\beta-2)} ((a/\pi)^{2-3\beta} - 1) \end{aligned} \quad (\text{S52})$$

$$= \boxed{c_{X11} a^{2-3\beta} + c_{X12}} \quad (\text{S53})$$

$$\begin{aligned} \iint_{\mathcal{D}_Y} d\theta' d\theta'' \left(\frac{1}{\theta' (\theta' - \theta'')} \right)^\beta &= \frac{a^{2-2\beta}}{2(\beta-1)^2} \left\{ 2(\beta-1) B_{\frac{a}{\pi}}[2\beta-1, 1-\beta] \right. \\ &\quad - \pi^{-1/2} (\beta-1) \Gamma[1-\beta] \Gamma[\beta-1/2] - 1 \\ &\quad \left. + (1 - {}_2F_1 \left[\begin{matrix} 2(\beta-1), \beta \\ 2\beta-1 \end{matrix}; a/\beta \right]) (a/\pi)^{2\beta-2} \right\} \end{aligned} \quad (\text{S54})$$

$$\sim \boxed{c_{Y11} a^{2-2\beta} + c_{Y12}} \quad (\text{S55})$$

$$\begin{aligned} \iint_{\mathcal{D}_Y} d\theta' d\theta'' \left(\frac{\theta''^{2-\gamma}}{\theta' (\theta' - \theta'')} \right)^\beta &= \frac{a^{2-\gamma\beta}}{\gamma\beta-2} \left\{ B_1[1+2\beta-\gamma\beta, 1-\beta] \right. \\ &\quad - B_1[2\beta-1, 1-\beta] + B_{\frac{a}{\pi}}[2\beta-1, 1-\beta] \\ &\quad \left. - (a/\pi)^{\gamma\beta-2} B_{\frac{a}{\pi}}[1+2\beta-\gamma\beta, 1-\beta] \right\} \end{aligned} \quad (\text{S56})$$

$$\sim \boxed{c_{Y21} a^{2-\gamma\beta} + c_{Y22} a^{1+2\beta-\gamma\beta}} \quad (\text{S57})$$

$$\begin{aligned} \iint_{\mathcal{D}_Y} d\theta' d\theta'' \left(\frac{\theta''^{2-\gamma}}{\theta' (\theta' - \theta'')} \right)^\beta \ln \left(\frac{\zeta}{\theta''^\beta} \right) &= \frac{\beta a^{2-\beta\gamma} \pi^{1-2\beta}}{(\beta(\gamma-2)-1)(\beta\gamma-2)^2} \\ &\quad \times \left\{ \frac{4^{\beta-1}}{\pi^{\frac{3}{2}-2\beta}} (\beta(\gamma-2)-1) \Gamma[1-\beta] \Gamma \left[\beta - \frac{1}{2} \right] \right. \\ &\quad + \frac{\pi^{2\beta-1} \Gamma[1-\beta] \Gamma[-\gamma\beta+2\beta+2]}{\Gamma[-\gamma\beta+\beta+2]} \\ &\quad \times \left(\frac{1+(\gamma\beta-2)(H_{\beta(2-\gamma)} - H_{1+\beta-\gamma\beta})}{\beta(\gamma-2)-1} \right) \\ &\quad - a^{2\beta-1} \left(\frac{(\beta(\gamma-2)-1)}{2\beta-1} {}_2F_1 \left[\begin{matrix} \beta, 2\beta-1 \\ 2\beta \end{matrix}; \frac{a}{\pi} \right] \right. \\ &\quad \left. \frac{(\beta\gamma-2)}{\beta(\gamma-2)-1} {}_3F_2 \left[\begin{matrix} \beta, -\gamma\beta+2\beta+1, -\gamma\beta+2 \\ \beta+1-\gamma\beta+2\beta+2, -\gamma\beta+2\beta+2 \end{matrix}; \frac{a}{\pi} \right] \right. \\ &\quad \left. \left. + {}_2F_1 \left[\begin{matrix} \beta, \beta(-\gamma)+2\beta+1 \\ \beta(-\gamma)+2\beta+2 \end{matrix}; \frac{a}{\pi} \right] \right) \right\} \end{aligned} \quad (\text{S58})$$

$$\sim \boxed{c_{Y_{31}} a^{2-\gamma\beta} + c_{Y_{32}} a^{1+2\beta-\gamma\beta}} \quad (\text{S59})$$

$$\iint_{\mathcal{D}_Z} d\theta' d\theta'' \left(\frac{1}{\theta'(\theta' - \theta'')} \right)^\beta = \frac{a^{2-2\beta} - b^{2-2\beta}}{2(\beta-1)^2} = \boxed{c_{Z_{11}} a^{2-2\beta} + c_{Z_{12}} b^{2-2\beta}} \quad (\text{S60})$$

$$\iint_{\mathcal{D}_Z} d\theta' d\theta'' \left(\frac{\theta''^{2-\gamma}}{\theta'(\theta' - \theta'')} \right)^\beta = \frac{\Gamma[1-\beta]\Gamma[-\gamma\beta+2\beta+1] (b^{2-\beta\gamma} - a^{2-\beta\gamma})}{(\beta\gamma-2)\Gamma[-\gamma\beta+\beta+2]} \quad (\text{S61})$$

$$= \boxed{c_{Z_{21}} a^{2-\gamma\beta} + c_{Z_{22}} b^{2-\gamma\beta}} \quad (\text{S62})$$

$$\begin{aligned} \iint_{\mathcal{D}_Z} d\theta' d\theta'' \left(\frac{\theta''^{2-\gamma}}{\theta'(\theta' - \theta'')} \right)^\beta \ln \left(\frac{\zeta}{\theta''^\beta} \right) &= \frac{\Gamma[1+2\beta-\gamma\beta]\Gamma[1-\beta]\beta}{(\beta\gamma-2)\Gamma[2+\beta-\gamma\beta]} (a^{2-\gamma\beta} - b^{2-\gamma\beta}) \\ &\times \left\{ H_{\beta(2-\gamma)} - H_{1+\beta-\gamma\beta} + \frac{1}{\gamma\beta-2} - \frac{1}{\beta} \log(\zeta) \right. \\ &\left. + \frac{a^{2-\gamma\beta} \log a - b^{2-\gamma\beta} \log b}{a^{2-\gamma\beta} - b^{2-\gamma\beta}} \right\} \quad (\text{S63}) \end{aligned}$$

$$= \boxed{a^{2-\gamma\beta} \left(c_{Z_{31}} + c_{Z_{32}} \left(\log(a) - \frac{1}{\beta} \log(\zeta) \right) \right) - b^{2-\gamma\beta} \left(c_{Z_{31}} + c_{Z_{32}} \left(\log(b) - \frac{1}{\beta} \log(\zeta) \right) \right)} \quad (\text{S64})$$

The next step is to organise the different scalings (see Tab. (S1), where we have defined $c_{Y_i} = c_{Y_{1i}} + c_{Y_{2i}} + c_{Y_{3i}}$ and similarly for Z .) that were found and find which is dominant.

	$\zeta = \left(\frac{\kappa_0}{\kappa_s} \right)^2$	$\zeta = \left(\frac{\kappa_0 \kappa_c}{\kappa_s^2} \right)^2$	$\zeta = \left(\frac{\kappa_c}{\kappa_s} \right)^2 \quad (\kappa_c \gg \kappa_s)$	$\zeta = \left(\frac{\kappa_c}{\kappa_s} \right)^2 \quad (\kappa_c \leq \kappa_s)$
X	$c_{X_{11}} \left(\frac{\kappa_0}{\kappa_s} \right)^{\frac{4}{\beta}-2\gamma} +$ $c_{X_{12}} \left(\frac{\kappa_0}{\kappa_s} \right)^{2(3-\gamma)}$	$c_{X_{11}} \left(\frac{\kappa_0 \kappa_c}{\kappa_s^2} \right)^{\frac{2}{\beta}-\gamma} +$ $c_{X_{12}} \left(\frac{\kappa_0 \kappa_c}{\kappa_s^2} \right)^{3-\gamma}$		$c_{X_{11}} \left(\frac{\kappa_c}{\kappa_s} \right)^{\frac{4}{\beta}-2\gamma} +$ $c_{X_{12}} \left(\frac{\kappa_c}{\kappa_s} \right)^{2(3-\gamma)}$
Y	$c_{Y1} \left(\frac{\kappa_0}{\kappa_s} \right)^{\frac{4}{\beta}-2\gamma} +$ $c_{Y2} \left(\frac{\kappa_0}{\kappa_s} \right)^{4+\frac{2}{\beta}-2\gamma}$	$c_{Y1} \left(\frac{\kappa_0 \kappa_c}{\kappa_s^2} \right)^{\frac{2}{\beta}-\gamma} +$ $c_{Y2} \left(\frac{\kappa_0 \kappa_c}{\kappa_s^2} \right)^{2+1/\beta-\gamma}$		$c_{Y1} \left(\frac{\kappa_c}{\kappa_s} \right)^{\frac{4}{\beta}-2\gamma} +$ $c_{Y2} \left(\frac{\kappa_c}{\kappa_s} \right)^{4+2/\beta-2\gamma}$
Z		$c_{Z1} \left(\frac{\kappa_0 \kappa_c}{\kappa_s^2} \right)^{\frac{2}{\beta}-\gamma} +$ $(c_{Z_{22}} - c_{Z_{31}}) \left(\frac{\kappa_0}{\kappa_s} \right)^{\frac{4}{\beta}-2\gamma} +$ $\frac{c_{Z_{32}}}{\beta} \left(\frac{\kappa_0}{\kappa_s} \right)^{\frac{4}{\beta}-2\gamma} \ln \left(\frac{\kappa_c}{\kappa_0} \right) +$ $c_{Z_{12}} \left(\frac{\kappa_0 \kappa_c}{\kappa_s^2} \right)^{2-\gamma} \left(\frac{\kappa_0}{\kappa_s} \right)^{\frac{4}{\beta}-4}$	$c_{Z_{11}} \pi^{2-2\beta} \left(\frac{\kappa_c}{\kappa_s} \right)^{2(2-\gamma)} +$ $(c_{Z_{21}} + c_{Z_{31}}) \pi^{2-\gamma\beta} +$ $(c_{Z_{22}} - c_{Z_{32}}) \left(\frac{\kappa_0}{\kappa_s} \right)^{\frac{4}{\beta}-2\gamma} -$ $\frac{2}{\beta} c_{Z_{32}} \pi^{2-\gamma\beta} \ln \left(\frac{\kappa_c}{\kappa_s} \right) +$ $\frac{2}{\beta} c_{Z_{32}} \left(\frac{\kappa_0}{\kappa_s} \right)^{\frac{4}{\beta}-2\gamma} \ln \left(\frac{\kappa_c}{\kappa_0} \right) +$ $c_{Z_{23}} \pi^{2-\gamma\beta} \ln(\pi) +$ $c_{Z_{12}} \left(\frac{\kappa_c}{\kappa_s} \right)^{2(2-\gamma)} \left(\frac{\kappa_0}{\kappa_s} \right)^{\frac{4}{\beta}-4}$	$c_{Z1} \left(\frac{\kappa_c}{\kappa_s} \right)^{\frac{4}{\beta}-2\gamma} +$ $(c_{Z_{22}} - c_{Z_{31}}) \left(\frac{\kappa_0}{\kappa_s} \right)^{\frac{4}{\beta}-2\gamma} +$ $\frac{2c_{Z_{32}}}{\beta} \left(\frac{\kappa_0}{\kappa_s} \right)^{\frac{4}{\beta}-2\gamma} \ln \left(\frac{\kappa_c}{\kappa_0} \right) +$ $c_{Z_{12}} \left(\frac{\kappa_c}{\kappa_s} \right)^{4-2\gamma} \left(\frac{\kappa_0}{\kappa_s} \right)^{\frac{4}{\beta}-4}$

TABLE S1. The different terms resulting from (S46).

Let us note that as the final results contains $I_{\kappa_c^2/\kappa_s^2} - 2I_{\kappa_0\kappa_c/\kappa_s^2}$, the terms containing $\ln(\kappa_c/\kappa_0)$ cancel. We now have many different scaling behaviours, and the question of which one dominates again depends on the value of β as well as κ_c . As a matter of fact, if one includes the κ_s^{-2} pre-factor in Eq. (S46), one recovers the same behaviour as was found for the lower bound

$$A_{-,l} \leq \begin{cases} C_{-,1} N^{-2/\beta+\gamma-1} + C_{-,2} N^{-1} \ln N & \text{if } \kappa_c \gg \kappa_s \\ N^{-1} \left(C_{-,3} N^{\gamma-2/\beta} + C_{-,4} N^{(1-\alpha)(\gamma-2/\beta)} + C_{-,5} N^{(1-\alpha)(\gamma-3)} \right) & \text{if } \kappa_c \leq \kappa_s \end{cases}, \quad (\text{S65})$$

where $C_{-,i}$ are constants.

This seems to go in the right direction. However, we have not explored the full integration domain yet. It turns out though that the integration domain \mathcal{D}_s does not lead to any new scaling:

$$\begin{aligned}
I_{-,s} &= \iint dx dy (xy)^{-\gamma} \iint_{\mathcal{D}_s} \frac{1}{1 + \frac{\theta'^\beta \kappa_s}{\kappa x}} \frac{1}{1 + \frac{\theta''^\beta \kappa_s}{\kappa y}} \frac{1}{1 + \frac{(\theta' - \theta'')^\beta}{xy}} \\
&\leq \iint dx dy (xy)^{-\gamma} \iint_{\mathcal{D}_s} 1 \\
&= \left(\frac{\kappa_0}{\kappa_s}\right)^{4/\beta} \iint dx dy (xy)^{-\gamma} \\
&= \left(\frac{\kappa_0}{\kappa_s}\right)^{4/\beta} \frac{1}{(1-\gamma)^2} \left(\left(\frac{\kappa_c}{\kappa_s}\right)^{1-\gamma} - \left(\frac{\kappa_0}{\kappa_s}\right)^{1-\gamma} \right)^2 \\
&\sim \frac{1}{(1-\gamma)^2} \left(\frac{\kappa_0}{\kappa_s}\right)^{2(1-\gamma+2/\beta)} \\
&\sim N^{-1+\gamma-2/\beta}.
\end{aligned} \tag{S66}$$

The contribution of \mathcal{D}_s is thus subleading for small β and equally dominant as the other contributions for large β . We have thus shown that for the the upper and lower bound the dominant scaling is the same. We now have the scaling of all distinct parts, B, A_+, A_- , so we can now combine them all.

$$C \sim \begin{cases} C_1 N^{2-2/\beta} + C_2 N^{2-\gamma} \ln N & \text{if } \kappa_c \gg \kappa_s \\ C_3 N^{2-2/\beta} + C_4 N^{2-2/\beta-\alpha(\gamma-2/\beta)} + C_5 N^{-1-\alpha(\gamma-3)} & \text{if } \kappa_c \leq \kappa_s \end{cases} \tag{S67}$$

Let us discuss the limiting cases of α . When $\alpha = 0$, $\kappa_0 \approx \kappa_c$, and the network thus has a homogeneous degree distribution. Then, $C \sim (C_3 + C_4) N^{2-2/\beta} + C_5 N^{-1}$. If $\alpha = 1$, i.e. $\kappa_c \approx \kappa_s$, the scaling becomes $C \sim C_3 N^{2-2/\beta} + (C_4 + C_5) N^{2-\gamma}$.

3. Case $\beta = 1$

We now turn to the limit $\beta = 1$. We know that in this case μ scales as $\hat{\mu} \sim (\ln N)^{-1}$ instead of $\hat{\mu} \sim N^{1-\beta}$, and thus $\kappa_s \sim \sqrt{N \ln N}$, which of course alters scaling. However, there might be more differences. We will represent all integrals evaluated at $\beta = 1$ by a tilde ($\tilde{A}_-, \tilde{A}_+, \tilde{B}$). We start with \tilde{B} :

$$\begin{aligned}
\tilde{B} &= \pi \left(\frac{\kappa_c}{\kappa_s}\right)^{1-\gamma} \int_0^1 d\theta \int_{\kappa_0/\kappa_c}^1 dx \frac{x^{-\gamma}}{1 + \frac{\pi\theta\kappa_s^2}{\kappa_c\kappa x}} \\
&= \pi \left(\frac{\kappa_c}{\kappa_s}\right)^{1-\gamma} \left\{ \frac{\kappa\kappa_c}{\pi\kappa_s^2} \frac{\log\left(1 + \frac{\pi\kappa_s^2}{\kappa_c\kappa}\right)}{2-\gamma} + \frac{1}{\gamma-2} \left(\frac{\kappa_0}{\kappa_c}\right)^{2-\gamma} \frac{\kappa\kappa_c}{\pi\kappa_s^2} \log\left(1 + \frac{\pi\kappa_s^2}{\kappa\kappa_0}\right) \right. \\
&\quad \left. + \frac{1}{(\gamma-2)(\gamma-1)} \left({}_2F_1\left[1, \gamma-1; \gamma; -\frac{\pi\kappa_s^2}{\kappa\kappa_c}\right] - \left(\frac{\kappa_0}{\kappa_c}\right)^{1-\gamma} {}_2F_1\left[1, \gamma-1; \gamma; -\frac{\pi\kappa_s^2}{\kappa\kappa_0}\right] \right) \right\}.
\end{aligned} \tag{S68}$$

The second term is dominant and thus B scales as

$$\tilde{B} \sim \kappa_s^{\gamma-3} \log(\kappa_s) \sim N^{\frac{\gamma-3}{2}} (\log N)^{\frac{\gamma-1}{2}}. \tag{S69}$$

For the lower bound of the numerator of the clustering coefficient we can use the result found in Eq. (S45) as nowhere was it assumed that $\beta < 1$. Irrespective of κ_c this gives us

$$\tilde{A}_+ \leq \tilde{c}_+ N^{\gamma-3} (\ln N)^{\gamma-3}. \tag{S70}$$

For the upper bound of \tilde{A}_- we cannot follow the same path as was done in the case of general β . This is because the upper bound employed, given by Eq. (S46), diverges in the $\beta = 1$ limit. Thus, we must find a stricter bound. This is done by once again dividing the angular integration domain, this time in four pieces: $\mathcal{D}_s = [0, (\kappa_0/\kappa_s)^2] \times [0, \theta']$, $\mathcal{D}_2 = [(\kappa_0/\kappa_s)^2, \pi] \times [0, (\kappa_0/\kappa_s)^2]$, $\mathcal{D}_3 = [(\kappa_0/\kappa_s)^2, \pi] \times [\theta' - (\kappa_0/\kappa_s)^2, \theta']$ and $\mathcal{D}_4 = [2(\kappa_0/\kappa_s)^2, \pi] \times [(\kappa_0/\kappa_s)^2, \theta' - (\kappa_0/\kappa_s)^2]$, as represented in Fig. S2

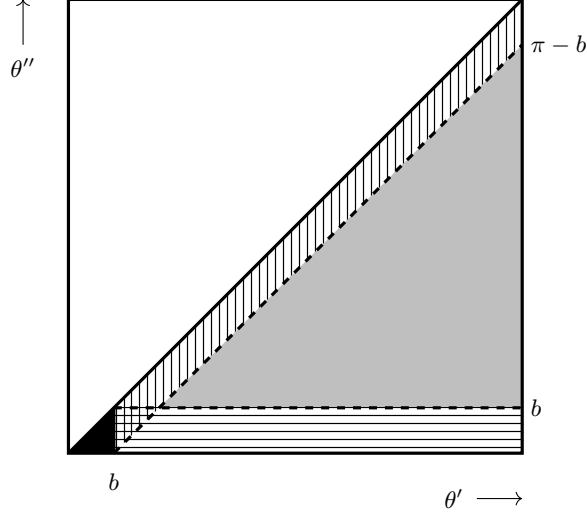


FIG. S2. Integration regions where $b = \frac{\kappa_0^2}{\kappa_s^2}$. The black region is region \mathcal{D}_s . The horizontally striped region is region \mathcal{D}_2 . The vertically striped region is region \mathcal{D}_3 . The grey region is region \mathcal{D}_4 .

Note that regions \mathcal{D}_2 and \mathcal{D}_3 overlap, but that is not a problem as our integrand is positive and counting a region double just increases the value of the integral, which in turn work for our purposes as we are only looking for an upper bound. For the region \mathcal{D}_s we can use the result (S66):

$$\tilde{A}_{-,s} \leq \tilde{c}_{-,s} N^{\gamma-3} (\ln N)^{\gamma-3}. \quad (\text{S71})$$

Turning to \mathcal{D}_2 we obtain

$$\begin{aligned} \tilde{A}_{-,2} &= \iint dx dy (xy)^{-\gamma} \iint_{\mathcal{D}_2} \frac{d\theta' d\theta''}{1 + \frac{\theta' \kappa_s}{\kappa x}} \frac{1}{1 + \frac{\theta'' \kappa_s}{\kappa y}} \frac{1}{1 + \frac{\theta' - \theta''}{xy}} \\ &\leq \frac{\kappa}{\kappa_s} \iint_{\mathcal{D}_2} \frac{d\theta' d\theta''}{\theta'} \int_{\kappa_s/\kappa_c}^{\kappa_s/\kappa_0} dx \int_{\kappa_s/\kappa_c}^{\kappa_s/\kappa_0} dy \frac{x^{\gamma-3} y^{\gamma-2}}{1 + xy(\theta' - \theta'')} \end{aligned} \quad (\text{S72})$$

where we have bounded the integral by decreasing the size of the denominators of the first and second terms. We also performed a change of variables of x and y . We now extend the lower bounds of the x and y integrals to zero, which can be done as our integral is positive, and so the resulting integral will be larger or equal to the original one.

$$\begin{aligned} \tilde{A}_{-,2} &\leq \frac{\kappa}{\kappa_s} \iint_{\mathcal{D}_2} \frac{d\theta' d\theta''}{\theta'} \int_0^{\kappa_s/\kappa_0} dx \int_0^{\kappa_s/\kappa_0} dy \frac{x^{\gamma-3} y^{\gamma-2}}{1 + xy(\theta' - \theta'')} \\ &= \frac{\kappa}{\kappa_s} (\kappa_s/\kappa_0)^{2\gamma-3} \iint_{\mathcal{D}_2} \frac{d\theta' d\theta''}{\theta'} \left(\Phi \left[-\frac{\kappa_s^2}{\kappa_0^2} (\theta' - \theta''), 1, \gamma - 2 \right] - \Phi \left[-\frac{\kappa_s^2}{\kappa_0^2} (\theta' - \theta''), 1, \gamma - 1 \right] \right) \end{aligned} \quad (\text{S73})$$

We know again have the situation that depending on the values of the angular coordinates, the arguments of the Φ 's diverge or go to zero. For the region $\mathcal{D}_{2s} = [b, 2b] \times [0, b]$, $\theta' - \theta'' \in [0, b]$, so the argument lies between zero and one. For the region $\mathcal{D}_{2l} = [2b, \pi] \times [0, b]$, $\theta' - \theta'' \in [b, \pi]$, so the argument is larger than one. We first turn to the second region. Here the argument can diverge and we should thus perform a similar transformation as Eq. (S48). It is not

exactly the same as the second argument of the Φ 's is now 1 and not two 2, but the derivation is equivalent. This leads us to

$$\begin{aligned}
& \frac{\kappa}{\kappa_s} (\kappa_s/\kappa_0)^{2\gamma-3} \iint_{\mathcal{D}_{2l}} \frac{d\theta' d\theta''}{\theta'} \left(\Phi \left[-\frac{\kappa_s^2}{\kappa_0^2} (\theta' - \theta''), 1, \gamma - 2 \right] - \Phi \left[-\frac{\kappa_s^2}{\kappa_0^2} (\theta' - \theta''), 1, \gamma - 1 \right] \right) \\
&= \frac{\kappa}{\kappa_s} (\kappa_s/\kappa_0)^{2\gamma-3} \iint_{\mathcal{D}_{2l}} \frac{d\theta' d\theta''}{\theta'} \left(\left(\frac{\kappa_s^2}{\kappa_0^2} (\theta' - \theta'') \right)^{2-\gamma} (\Phi[-1, 1, 3 - \gamma] + \Phi[-1, 1, 2 - \gamma]) \right. \\
&\quad - \left(\frac{\kappa_s^2}{\kappa_0^2} (\theta' - \theta'') \right)^{-1} \Phi \left[-\left(\frac{\kappa_s^2}{\kappa_0^2} (\theta' - \theta'') \right)^{-1}, 1, 3 - \gamma \right] \\
&\quad + \left(\frac{\kappa_s^2}{\kappa_0^2} (\theta' - \theta'') \right)^{1-\gamma} (\Phi[-1, 1, 2 - \gamma] + \Phi[-1, 1, 1 - \gamma]) \\
&\quad \left. - \left(\frac{\kappa_s^2}{\kappa_0^2} (\theta' - \theta'') \right)^{-1} \Phi \left[-\left(\frac{\kappa_s^2}{\kappa_0^2} (\theta' - \theta'') \right)^{-1}, 1, 2 - \gamma \right] \right) \\
&\leq \frac{\kappa}{\kappa_s} (\kappa_s/\kappa_0)^{2\gamma-3} \iint_{\mathcal{D}_{2l}} \frac{d\theta' d\theta''}{\theta'} \left(\left(\frac{\kappa_s^2}{\kappa_0^2} (\theta' - \theta'') \right)^{2-\gamma} (\Phi[-1, 1, 3 - \gamma] + \Phi[-1, 1, 2 - \gamma]) \right. \\
&\quad + \left(\frac{\kappa_s^2}{\kappa_0^2} (\theta' - \theta'') \right)^{1-\gamma} (\Phi[-1, 1, 2 - \gamma] + \Phi[-1, 1, 1 - \gamma]) \\
&\quad \left. - 2 \left(\frac{\kappa_s^2}{\kappa_0^2} (\theta' - \theta'') \right)^{-1} \right) \sim \kappa_s^{2(\gamma-3)} \sim N^{\gamma-3} (\ln N)^{\gamma-3}. \tag{S74}
\end{aligned}$$

For \mathcal{D}_{2s} we can immediately bound away the Φ to find

$$\begin{aligned}
& \frac{\kappa}{\kappa_s} (\kappa_s/\kappa_0)^{2\gamma-3} \iint_{\mathcal{D}_{2s}} \frac{d\theta' d\theta''}{\theta'} \left(\Phi \left[-\frac{\kappa_s^2}{\kappa_0^2} (\theta' - \theta''), 1, \gamma - 2 \right] - \Phi \left[-\frac{\kappa_s^2}{\kappa_0^2} (\theta' - \theta''), 1, \gamma - 1 \right] \right) \\
&\leq \frac{\kappa}{\kappa_s} (\kappa_s/\kappa_0)^{2\gamma-3} \iint_{\mathcal{D}_{2s}} \frac{d\theta' d\theta''}{\theta'} = \frac{\kappa}{\kappa_s} (\kappa_s/\kappa_0)^{2\gamma-5} \ln 2 \sim N^{\gamma-3} (\ln N)^{\gamma-3}. \tag{S75}
\end{aligned}$$

Combining the two results we find that $\tilde{A}_{-,2} \leq I \sim N^{\gamma-3} (\ln N)^{\gamma-3}$, where I is some integral, as expected. Then we investigate to \mathcal{D}_3 :

$$\begin{aligned}
\tilde{A}_{-,3} &= \iint dx dy (xy)^{-\gamma} \iint_{\mathcal{D}_3} d\theta' d\theta'' \frac{1}{1 + \frac{\theta' \kappa_s}{\kappa x}} \frac{1}{1 + \frac{\theta'' \kappa_s}{\kappa y}} \frac{1}{1 + \frac{\theta' - \theta''}{xy}} \\
&= \iint dx dy (xy)^{-\gamma} \iint_{\mathcal{D}_2} d\theta' d\theta'' \frac{1}{1 + \frac{\theta' \kappa_s}{\kappa x}} \frac{1}{1 + \frac{(\theta' - \theta'') \kappa_s}{\kappa y}} \frac{1}{1 + \frac{\theta''}{xy}} \\
&\leq \left(\frac{\kappa}{\kappa_s} \right)^2 \iint dx dy x^{1-\gamma} y^{1-\gamma} \iint_{\mathcal{D}_2} d\theta' d\theta'' \frac{1}{\theta'} \frac{1}{\theta' - \theta''} \\
&= \frac{1}{(2-\gamma)^2} \left(\frac{\kappa}{\kappa_s} \right)^2 \left(\frac{\kappa_0}{\kappa_s} \right)^{2(2-\gamma)} \left(\frac{\pi^2}{6} - \text{Li}_2 \left[\frac{\kappa_0^2}{\kappa_s^2 \pi} \right] \right) \\
&\sim \kappa_s^{2(\gamma-3)} \sim N^{\gamma-3} (\ln N)^{\gamma-3}. \tag{S76}
\end{aligned}$$

Here $\text{Li}_2(z)$ is the dilogarithm. The final region to be studied is \mathcal{D}_4 :

$$\begin{aligned}
\tilde{A}_{-,4} &= \iint dx dy (xy)^{-\gamma} \iint_{\mathcal{D}_4} d\theta' d\theta'' \frac{1}{1 + \frac{\theta' \kappa_s}{\kappa x}} \frac{1}{1 + \frac{\theta'' \kappa_s}{\kappa y}} \frac{1}{1 + \frac{\theta' - \theta''}{xy}} \\
&\leq \left(\frac{\kappa}{\kappa_s} \right)^2 \iint dx dy (xy)^{1-\gamma} \iint_{\mathcal{D}_4} d\theta' d\theta'' \frac{1}{\theta' \theta''} \frac{1}{1 + \frac{\theta' - \theta''}{xy}}
\end{aligned}$$

$$\begin{aligned}
&= \left(\frac{\kappa}{\kappa_s}\right)^2 \int_{\kappa_s/\kappa_c}^{\kappa_s/\kappa_0} dx \int_{\kappa_s/\kappa_c}^{\kappa_s/\kappa_0} dy (xy)^{\gamma-3} \iint_{\mathcal{D}_4} d\theta' d\theta'' \frac{1}{\theta'\theta''} \frac{1}{1+xy(\theta'-\theta'')} \\
&\leq \left(\frac{\kappa}{\kappa_s}\right)^2 \int_0^{\kappa_s/\kappa_0} dx \int_0^{\kappa_s/\kappa_0} dy (xy)^{\gamma-3} \iint_{\mathcal{D}_4} d\theta' d\theta'' \frac{1}{\theta'\theta''} \frac{1}{1+xy(\theta'-\theta'')} \\
&= \left(\frac{\kappa}{\kappa_s}\right)^2 \left(\frac{\kappa_s}{\kappa_0}\right)^{2(\gamma-2)} \iint_{\mathcal{D}_4} d\theta' d\theta'' \frac{1}{\theta'\theta''} \Phi \left[-\frac{\kappa_s^2}{\kappa_0^2}(\theta'-\theta''), 2, \gamma-2 \right] \\
&\leq \left(\frac{\kappa}{\kappa_s}\right)^2 \iint_{\mathcal{D}_4} d\theta' d\theta'' \frac{1}{\theta'\theta''} \left\{ (\theta'-\theta'')^{2-\gamma} \left[\Psi(\cdot) \log \left(\frac{\kappa_s^2}{\kappa_0^2}(\theta'-\theta'') \right) + \vartheta(\cdot) \right] \right. \\
&\quad \left. + \left(\frac{\kappa_s}{\kappa_0}\right)^{2(\gamma-3)} (\theta'-\theta'')^{-1} (3-\gamma)^{-2} \right\}. \tag{S77}
\end{aligned}$$

Let us investigate the term with the logarithm first.

$$\begin{aligned}
&\left(\frac{\kappa}{\kappa_s}\right)^2 \int_{2\kappa_0^2/\kappa_s^2}^{\pi} d\theta' \int_{\kappa_0^2/\kappa_s^2}^{\theta'-\kappa_0^2/\kappa_s^2} d\theta'' \frac{(\theta'-\theta'')^{2-\gamma}}{\theta'\theta''} \log \left(\frac{\kappa_s^2}{\kappa_0^2}(\theta'-\theta'') \right) \\
&= \left(\frac{\kappa}{\kappa_s}\right)^2 \left(\frac{\kappa_0}{\kappa_s}\right)^{2(2-\gamma)} \int_2^{\pi\kappa_s^2/\kappa_0^2} d\theta' \int_1^{\theta'-1} d\theta'' \frac{(\theta'-\theta'')^{2-\gamma}}{\theta'\theta''} \log(\theta'-\theta'') \\
&= \left(\frac{\kappa}{\kappa_s}\right)^2 \left(\frac{\kappa_0}{\kappa_s}\right)^{2(2-\gamma)} \int_2^{\pi\kappa_s^2/\kappa_0^2} d\theta' \int_1^{\theta'-1} d\theta'' \frac{(\theta'')^{2-\gamma}}{\theta'(\theta'-\theta'')} \log(\theta''). \tag{S78}
\end{aligned}$$

This can then be evaluated. The θ'' integral leads to a variety of different terms, that need to be treated separately. Some variable transformations need to be performed, and some special functions need to be expanded to their series representation. It can be shown that the integral to leading order is constant in N , implying that the logarithm term of $\tilde{A}_{-,4}$ scales as $\kappa_s^{2(\gamma-3)}$. The other two terms in expression (S77) are easier to evaluate:

$$\begin{aligned}
\iint_{\mathcal{D}_4} d\theta' d\theta'' \frac{1}{\theta'\theta''} (\theta'-\theta'')^{2-\gamma} &= \frac{(b^{2-\gamma} + \pi^{2-\gamma})}{\gamma-2} \left\{ B_{1-\frac{b}{\pi}}[3-\gamma, \gamma-2] - B_{\frac{1}{2}}[3-\gamma, \gamma-2] \right\} \\
&\quad + \frac{b^{2-\gamma} \ln(2-\frac{2b}{\pi})}{\gamma-2} \sim \left(\frac{\kappa_0}{\kappa_s}\right)^{2(2-\gamma)} \tag{S79}
\end{aligned}$$

$$\iint_{\mathcal{D}_4} d\theta' d\theta'' \frac{1}{\theta'\theta''} (\theta'-\theta'')^{-1} = \frac{2 \log(2-\frac{2b}{\pi})}{b} - \frac{2 \log(\frac{\pi}{b}-1)}{\pi} \sim \frac{\kappa_s^2}{\kappa_0^2}. \tag{S80}$$

Plugging this back in we find that also the integral over the region \mathcal{D}_4 scales as $N^{\gamma-3}(\ln N)^{\gamma-3}$.

Thus, we can finally conclude that for $\beta = 1$, the clustering coefficient must scale as

$$\boxed{C \sim \frac{N^{\gamma-3}(\log N)^{\gamma-3}}{N^{\gamma-3}(\log N)^{\gamma-1}} = (\log N)^{-2}}. \tag{S81}$$

With this we have found the critical exponent $\eta/\nu = 2$.

D. Exponent η

In this section we show that the scaling exponent η that encodes how the clustering approaches zero when $\beta \rightarrow \beta_c^+ = 1$. As this only requires working on the low temperature side of the transition, we can directly work in the thermodynamic limit. To this end, we denote the general definition of the clustering coefficient with hidden degree κ and (without loss of generality) spacial coordinate $r = 0$

$$C(\kappa) = \frac{\int_{\kappa_0}^{\infty} d\kappa' \int_{\kappa_0}^{\infty} d\kappa'' \int_{-\infty}^{\infty} dr' \int_{-\infty}^{\infty} dr'' \rho(\kappa') \rho(\kappa'') F(\kappa, \kappa', |r'|) F(\kappa, \kappa'', |r''|) F(\kappa', \kappa'', |r' - r''|)}{\left(\int_{\kappa_0}^{\infty} d\kappa' \int_{-\infty}^{\infty} dr' \rho(\kappa') F(\kappa, \kappa', |r'|) \right)^2}. \quad (\text{S82})$$

where we can use connection probability (S8) and $\hat{\mu}$ (S9).

Let us first turn to the denominator:

$$\int d\kappa' \rho(\kappa') \int_{-\infty}^{\infty} \frac{dr'}{1 + \left(\frac{r'}{\kappa \kappa' \hat{\mu}}\right)^\beta} = \kappa, \quad (\text{S83})$$

where we have plugged in the definition of $\hat{\mu}$ and used that $\langle k \rangle = \frac{\gamma-1}{\gamma-2} \kappa_0$.

The next step is the numerator. We first perform the transformation $t = r' / (\kappa \kappa' \hat{\mu})$ and $\tau = r'' / (\kappa \kappa'' \hat{\mu})$ to obtain

$$C(\kappa) = \frac{\hat{\mu}^2}{4} (\gamma - 1)^2 \kappa_0^{2\gamma-2} \iiint\!\!\!\int d\kappa' d\kappa'' dt d\tau \frac{(\kappa' \kappa'')^{1-\gamma}}{1 + |t|^\beta} \frac{1}{1 + |\tau|^\beta} \frac{1}{1 + \left|\frac{\kappa t}{\kappa'} - \frac{\kappa \tau}{\kappa''}\right|^\beta}. \quad (\text{S84})$$

We know that $\hat{\mu}^2 \sim (\beta - 1)^2 + \mathcal{O}((\beta - 1)^3)$. This is exactly the scaling that we expect from numerical investigation for the clustering coefficient. Thus, all we need to prove is that at $\beta = 1$, the numerator is finite. If so, its $(\beta - 1)$ dependence must be order $\mathcal{O}(1)$. If the full expression contained $(\beta - 1)^{-n}$ terms with $n > 0$ it would diverge at the critical point and if the dominant term was $\mathcal{O}((\beta - 1)^n)$ with $n > 0$ the numerator would go to zero at the critical point. And indeed, numerical integration shows that at $\beta = 1$ the numerator is finite, leading to the conclusion that

$$\boxed{C(\kappa) \sim (\beta - 1)^2} \quad (\text{S85})$$

such that $\eta = 2$, which in turn implies that $\nu = 1$.

II. REAL NETWORKS

As was stated in the main text, the DPG algorithm can be used to find the temperature of its embedding in the \mathbb{S}_1 model. We list here a collection of real networks and their corresponding inverse temperatures. We choose to restrict ourselves to models where the inverse temperature lies below or close to the transition point β_c .

Network Names	Type	$ V $	$ E $	$\langle k \rangle$	Target C	β
CElegans-C [5]	Biological - Brain	279	2287	16	0.34	1.5
Drosophila1-C [6]	Biological - Brain	350	2887	16	0.25	1.1
Drosophila2-C [6]	Biological - Brain	1770	8905	10	0.33	1.1
Arabidopsis-G [7]	Biological - Cell	4519	10721	4.7	0.16	1.2
CElegans-G [5]	Biological - Cell	3692	7650	4.2	0.11	0.77
Drosophila-G [8]	Biological - Cell	8114	38909	9.6	0.12	1.1
Human1-P [9]	Biological - Cell	913	7472	16	0.23	1.0
Human2-P [9]	Biological - Cell	1090	9369	17	0.20	1.0
Mus-G [8]	Biological - Cell	7402	16858	4.6	0.13	1.1
Rattus-G [8]	Biological - Cell	2350	3484	3.0	0.22	0.74
Yeast1-P [10]	Biological - Cell	1647	2518	3.1	0.10	1.2
Yeast2-P [11]	Biological - Cell	1458	1948	2.7	0.14	1.5
Polblogs-H [12]	Citation - Hyperlinks	1222	16714	27	0.36	1.1
Wiki-H [13]	Citation - Hyperlinks	1872	15367	16	0.42	1.3
Ecological [14]	Ecological - Troffic	700	6495	18	0.10	0.15
Commodities [15]	Economic - Commodities	374	1090	5.8	0.22	1.2
Friends-OFF [16]	Social Offline - Friends	2539	10455	8.2	0.15	1.4
Airports1 [17]	Transport - Flights	1572	17214	22	0.64	1.4

TABLE S2. Properties of a selection of networks with the inverse temperature β obtained with the DPG algorithm. Only networks with $\beta < 1.5$ are shown.

-
- [1] M. Boguñá and R. Pastor-Satorras, *Phys Rev E* **68**, 36112 (2003).
- [2] P. Colomer-de Simón and M. Boguñá, *Phys Rev E* **86**, 026120 (2012).
- [3] M. Boguñá, D. Krioukov, P. Almagro, and M. A. Serrano, *Phys. Rev. Research* **2**, 023040 (2020).
- [4] Note that we use a slightly different form than the standard ${}_2F_1[a, b; c; z]$ for aesthetic purposes.
- [5] Y.-Y. Ahn, H. Jeong, and B. J. Kim, *Physica A: Statistical Mechanics and its Applications* **367**, 531 (2006).
- [6] S.-y. Takemura, A. Bharioke, T. Zhao, J. A. Horne, R. D. Fetter, S. Takemura, K. Blazek, L.-A. Chang, O. Ogundeyi, M. A. Saunders, V. Shapiro, C. Sigmund, Z. Lu, G. M. Rubin, L. K. Scheffer, I. A. Meinertzhagen, D. B. Chklovskii, A. Nern, S. Vitaladevuni, P. K. Rivlin, W. T. Katz, D. J. Olbris, S. M. Plaza, and P. Winston, *Nature* **500**, 175 (2013).
- [7] A. Consortium, *Science* **333**, 601 (2011).
- [8] C. Stark, B.-J. Breitkreutz, T. Reguly, L. Boucher, A. Breitkreutz, and M. Tyers, *Nucleic Acids Research* **34**, D535 (2006).
- [9] A. Chang, I. Schomburg, S. Placzek, L. Jeske, M. Ulbrich, M. Xiao, C. W. Sensen, and D. Schomburg, *Nucleic Acids Research* **43**, D439 (2014).
- [10] H. Yu, P. Braun, M. A. Yıldırım, I. Lemmens, K. Venkatesan, J. Sahalie, T. Hirozane-Kishikawa, F. Gebreab, N. Li, N. Simonis, T. Hao, J.-F. Rual, A. Dricot, A. Vazquez, R. R. Murray, C. Simon, L. Tardivo, S. Tam, N. Svrzikapa, C. Fan, A.-S. de Smet, A. Motyl, M. E. Hudson, J. Park, X. Xin, M. E. Cusick, T. Moore, C. Boone, M. Snyder, F. P. Roth, A.-L. Barabási, J. Tavernier, D. E. Hill, and M. Vidal, *Science* **322**, 104 (2008).
- [11] Protein network dataset, KONECT (2007).
- [12] L. A. Adamic and N. Glance, *Proceedings of the 3rd international workshop on Link discovery*, 36–43 (2005).
- [13] B. Heaberlin and S. DeDeo, *Future Internet* **8** (2016).
- [14] J. A. Dunne, C. C. Labandeira, and R. J. Williams, *Proceedings of the Royal Society B: Biological Sciences* **281**, 20133280 (2014).
- [15] D. Grady, C. Thiemann, and D. Brockmann, *Nature communications* **3**, 864 (2012).
- [16] J. Moody, *Social Networks* **23**, 261 (2001).
- [17] T. Opsahl, Why anchorage is not (that) important: Binary ties and sample selection, <http://web.archive.org/web/20080207010024/http://www.808multimedia.com/winnt/kernel.htm> (2011), accessed: June 2021.